Monthly Notices
of the
ROYAL ASTRONOMICAL SOCIETY

MNRAS **436,** 705–717 (2013)
Advance Access publication 2013 September 25

doi:10.1093/mnras/stt1608

# Mirror, firehose and cosmic-ray-driven instabilities in a high-$\beta$ plasma

A. Achterberg★

*Department of Astrophysics, IMAPP, Radboud University, PO Box 9010, NL-6500 GL Nijmegen, the Netherlands*

Accepted 2013 August 22. Received 2013 August 6; in original form 2013 May 30

**ABSTRACT**

I consider low-frequency instabilities in a plasma with high-$\beta$ plasma, with $\beta$ the ratio of thermal and magnetic pressures. I derive the mirror and firehose instabilities, due to pressure anisotropy, for such a plasma. This derivation uncovers clear modifications with the more familiar, low-$\beta$ case. I also consider the interplay between these instabilities and the current-driven instability (the *Bell–Lucek instability*) that occurs near a shock that accelerates cosmic rays. It is shown that the two instability mechanisms in combination can lead to a stronger instability over a wider range of wavelengths.

**Key words:** acceleration of particles – diffusion – instabilities – shock waves – methods: waves.

## 1 INTRODUCTION

The properties of low-frequency magnetohydrodynamics (MHD) waves in high-$\beta$ plasmas, where $\beta \equiv 8\pi P/B^2$ is the ratio of the thermal and magnetic pressures, differ considerably from the properties obtained from a simple fluid approximation. In particular, the fundamental wave modes are coupled and through this coupling obliquely propagating Alfvén waves become subject to linear collisionless damping.

The first full calculation using kinetic theory of low-frequency quasi-MHD waves in such plasmas is due to Foote & Kulsrud (1979), building on earlier work by Stepanov (1958) and Barnes (1966). For frequencies well below the ion gyrofrequency $\Omega_\mathrm{i} = qB_0/m_\mathrm{i}c$ in the ambient magnetic field $B_0$, finite Larmor radius corrections to the ion response in the waves, as well as the effects of thermal motion along the magnetic field, change the character of the waves. In particular, the $\boldsymbol{E} \times \boldsymbol{B}_0$ drift speed (with $\boldsymbol{E}$ the electric field in the wave) of ions in a high-$\beta$ plasma differs from that of electrons as the mean wave electric field, averaged over one gyro-orbit, equals

$$\langle \boldsymbol{E}(\boldsymbol{k}) \rangle = \boldsymbol{E}(\boldsymbol{k})\, J_0\left(\frac{k_\perp v_\perp}{\Omega}\right) \simeq \boldsymbol{E}(\boldsymbol{k})\, \left(1 - \frac{k_\perp^2 v_\perp^2}{4\Omega^2}\right). \quad (1)$$

Here $v_\perp$ is the component of the particle velocity in the plane perpendicular to the ambient magnetic field and $k_\perp$ is the corresponding component of the wave vector $\boldsymbol{k}$, $\Omega = qB_0/mc$ is the gyrofrequency and $J_0$ is the Bessel function of order zero. The second equality assumes $k_\perp v_\perp/\Omega \ll 1$, the standard assumption for MHD waves that the wavelength is much larger than the gyroradius $r_\mathrm{g} = v_\perp/\Omega$ of all charge species in the plasma. This averaging procedure applies as long as the wave frequency is much lower than the ion gyrofrequency: $\omega \ll \Omega_\mathrm{i}$.

Assuming a plasma with similar ion and electron temperatures the mean square thermal velocity for particles of mass $m$ is equal to

$$\langle v_\perp^2 \rangle = \frac{2k_\mathrm{b}T_\perp}{m} \equiv 2V_\perp^2. \quad (2)$$

Using this estimate for $v_\perp^2$, together with $\Omega_\mathrm{i} = eB_0/m_\mathrm{i}c$ ($|\Omega_\mathrm{e}| = eB_0/m_\mathrm{e}c$) for ions (electrons) in a hydrogen plasma, one sees that the finite gyration radius correction in relation (1) is a factor $m_\mathrm{e}/m_\mathrm{p} \sim 1/1836$ smaller for electrons than it is for ions. The effect of the finite gyration radius on the electron response can therefore safely be neglected for realistic parameters. The difference in the ion and electron response leads to a net current associated with the $\boldsymbol{E} \times \boldsymbol{B}_0$ drift of both species. The standard MHD approximation applies to long wavelength modes in a plasma with sufficiently low $\beta$, where the correction to the ion response remains small and electrons and ions drift across the magnetic field with the same velocity.

In relation (2) I have allowed for the possibility that the plasma has a temperature anisotropy, where the temperature $T_\perp$ associated with the two degrees of freedom perpendicular to the magnetic field differs from the parallel temperature $T_\parallel$ associated with thermal motion along the magnetic field. The latter is defined formally by

$$\langle v_\parallel^2 \rangle = \frac{k_\mathrm{b}T_\parallel}{m} \equiv V_\parallel^2. \quad (3)$$

Thermal motion of the ions along the magnetic field also changes wave properties when $k_\parallel v_\parallel \simeq \Omega_\mathrm{i}$, with correction terms scaling as $k_\parallel^2 V_\parallel^2/\Omega_\mathrm{i}^2$, similar in form to those resulting from finite Larmor radius effects. Both effects are included in the calculations presented below.

Two well-known instabilities are associated with a temperature anisotropy and are discussed in this paper. I will derive the high-$\beta$ versions of the *firehose instability*, commonly associated with the Alfvén wave and the magnetosonic wave that propagate

★ E-mail: a.achterberg@astro.uu.nl

quasi-parallel along the field, and the *mirror instability* that is associated with a magnetosonic wave propagating quasi-perpendicular to the field. These two instabilities are receiving renewed interest with the realization that conditions in the interstellar/intergalactic medium are such that the low ion collision frequency allows anisotropies to develop in the ions distribution in the presence of weak magnetic fields (e.g. Schekochihin et al. 2005).

As will be demonstrated below in Section 6, the low ion collisionality allows for ion pressure anisotropies to be generated in the cosmic ray (CR) precursors of shocks that accelerate these particles by the shock acceleration mechanism. Instabilities in these precursors, driven by the return current induced by the streaming CRs in the plasma, have also been the subject of recent interest (Lucek & Bell 2000; Bell & Lucek 2001; Bell 2004; Luo & Melrose 2009). In the precursor the pressure force from of the accelerated CRs slows down the incoming fluid, and the resulting changes in the magnetic field and plasma density allow pressure anisotropies to develop in the ion plasma if the scattering rate of the thermal ions is sufficiently small.

This paper is organized as follows: the plasma response for low-frequency waves in an anisotropic quasi-Maxwellian high-$\beta$ plasma is calculated in Section 2. The wave properties and possible instabilities are discussed in Sections 3 and 4. The (indirect) effect of CRs is considered in Section 5, and in Sections 6 and 7 I discuss the application to the CR precursors in the high Mach number shocks that accelerate these particles. The conclusions are found in Section 8.

## 2 DISPERSION RELATION FOR QUASI-MHD WAVES

The calculation of linear wave properties in a plasma involves the determination of the dielectric tensor $\boldsymbol{\epsilon}(\omega,\ \boldsymbol{k})$ as a function of wave angular frequency $\omega$ and wave vector $\boldsymbol{k}$. It can be represented as

$$\boldsymbol{\epsilon}(\omega,\ \boldsymbol{k}) = \boldsymbol{I} + \sum_\sigma \boldsymbol{\chi}^\sigma(\omega,\ \boldsymbol{k}). \tag{4}$$

Here $\boldsymbol{\chi}^\sigma(\omega,\ \boldsymbol{k})$ is the susceptibility tensor of species $\sigma$, with $\sigma = \mathrm{e}, \mathrm{i}$ for a simple ion–electron plasma, and $\boldsymbol{I} = \mathrm{diag}(1,\ 1,\ 1)$ is the unit tensor. The dispersion relation of the waves that determines the frequency $\omega(\boldsymbol{k})$ as a function of wavenumber then reads, see for instance Ichimaru (1973), Akhiezer et al. (1975) and Stix (1992):

$$\det\left[\ \frac{k^2c^2}{\omega^2}\,(\boldsymbol{I} - \hat{\boldsymbol{\kappa}}\,\hat{\boldsymbol{\kappa}}) - \boldsymbol{\epsilon}(\omega,\ \boldsymbol{k})\ \right] \equiv \det[\ \boldsymbol{D}(\omega,\ \boldsymbol{k})\ ] = 0. \tag{5}$$

Here $\hat{\boldsymbol{\kappa}} \equiv \boldsymbol{k}/k$ is the unit vector along the wave vector. The second equality in this condition defines the dispersion tensor $\boldsymbol{D}(\omega,\ \boldsymbol{k})$. The dispersion relation is the solution condition for the set of coupled equations $\sum_{j=1}^3 D_{ij}(\omega,\ \boldsymbol{k})\ E_j(\omega,\ \boldsymbol{k}) = 0$ that follow from Maxwell's equations and the linearized equation of motion (or kinetic equation) for all components of the plasma.

Low-frequency MHD waves follow from a simplified version of dispersion relation (5). In what follows I choose the ambient magnetic field along the $z$-axis ($\boldsymbol{B}_0 = B_0\hat{\boldsymbol{z}}$) and the wave vector as $\boldsymbol{k} = k_\perp\hat{\boldsymbol{x}} + k_\parallel\hat{\boldsymbol{z}}$. For waves with a frequency much less than the electron plasma frequency $\omega_{\rm pe} = \sqrt{4\pi e^2 n_{\rm e}/m_{\rm e}}$ (with $n_{\rm e}$ the electron density) one can show that the component of the wave electric field along the magnetic field, $E_z(\omega,\ \boldsymbol{k})$, is almost shorted out by the electrons. This implies $D_{zz}$ is much larger than $D_{xx}$, $D_{yy}$, $D_{xy}$ and $D_{yx}$ and $|E_z| \ll |E_x|, |E_y|$. One can then limit the discussion to waves where the wave electric field lies entirely in the plane perpendicular to $\boldsymbol{B}_0$: $\boldsymbol{E}_\perp(\omega,\ \boldsymbol{k}) = \big(E_x(\omega,\ \boldsymbol{k}),\ E_y(\omega,\ \boldsymbol{k}),\ 0\big)$. The wave properties for such waves follow from the condition that the determinant of the cofactor of $D_{zz}$ vanishes (cf. Foote & Kulsrud 1979): $D_{xx}D_{yy} - D_{xy}D_{yx} = 0$. In terms of susceptibilities $\chi_{ij}(\omega,\ \boldsymbol{k})$:

$$\left(\frac{k_\parallel^2c^2}{\omega^2} - 1 - \chi_{xx}\right)\left(\frac{k^2c^2}{\omega^2} - 1 - \chi_{yy}\right) - \chi_{xy}^2 = 0. \tag{6}$$

### 2.1 Ion response

The susceptibility tensor $\boldsymbol{\chi}^\sigma(\omega,\ \boldsymbol{k})$ can be calculated by standard means. A convenient assumption is that the ion velocity distribution is a bi-Maxwellian $f_{\rm BM}(v_\perp, v_\parallel)$, where the number of ions found in the velocity interval $v_\parallel,\ v_\parallel + \mathrm{d}v_\parallel,\ v_\perp,\ v_\perp + \mathrm{d}v_\perp$ equals $\mathrm{d}n_{\rm i} \equiv n_{\rm i}\,f_{\rm BM}(v_\perp,\ v_\parallel)\,2\pi v_\perp \mathrm{d}v_\perp\,\mathrm{d}v_\parallel$, with

$$f_{\rm BM}(v_\perp,\ v_\parallel) = \frac{1}{(2\pi)^{3/2}\,V_\perp^2\,V_\parallel}\exp\left(-\frac{v_\perp^2}{2V_\perp^2} - \frac{v_\parallel^2}{2V_\parallel^2}\right). \tag{7}$$

Here the characteristic ion thermal speeds $V_\perp$ and $V_\parallel$ are defined in equations (2)/(3) in terms of the perpendicular (parallel) ion temperatures $T_\perp$ ($T_\parallel$). The quantity $n_{\rm i}$ is the total number density of the ions, and $v_\perp$ ($v_\parallel$) refer to the components of the particle velocity perpendicular to (along) the magnetic field. The ion plasma exhibits a temperature anisotropy if $T_\parallel \neq T_\perp$ ($V_\parallel \neq V_\perp$). To quantify this I introduce the ion anisotropy parameter:

$$\Delta_T = \frac{T_\perp}{T_\parallel} - 1 = \frac{P_\perp}{P_\parallel} - 1. \tag{8}$$

I have suppressed the species subscript 'i' on most quantities, concentrating for now on the ion contribution to the susceptibility.

The ion susceptibility tensor is (e.g. Ichimaru 1973, Ch. 5.2)

$$\boldsymbol{\chi}^{\rm i} = -\frac{\omega_{\rm pi}^2}{\omega^2}\left[\boldsymbol{I} + \sum_{n=-\infty}^{+\infty}\int \mathrm{d}v_\perp\mathrm{d}v_\parallel 2\pi v_\perp\left(\frac{\hat{G}_n\,f_{\rm BM}(v_\perp, v_\parallel)}{n\Omega_{\rm i} + k_\parallel v_\parallel - \omega}\right)\boldsymbol{\Pi}_n\right]. \tag{9}$$

Here $\omega_{\rm pi}^2 \equiv 4\pi e^2 n_{\rm i}/m_{\rm p}$ is the ion plasma frequency squared (assuming a hydrogen plasma with $q = e$ and $m = m_{\rm p}$), $\Omega_{\rm i} = eB_0/m_{\rm p}c$ is the ion gyrofrequency and $\hat{G}_n$ is the operator:

$$\hat{G}_n \equiv \frac{n\Omega_{\rm i}}{v_\perp}\,\frac{\partial}{\partial v_\perp} + k_\parallel\,\frac{\partial}{\partial v_\parallel}. \tag{10}$$

The $3 \times 3$ tensor $\boldsymbol{\Pi}_n$ involves products of Bessel functions and derivatives thereof. In the present case we only need the components $\Pi_{xx}$, $\Pi_{yy}$ and $\Pi_{xy} = -\Pi_{yx}$ in the plane perpendicular to $\boldsymbol{B}_0$, which together can be represented by the $2 \times 2$ matrix $\boldsymbol{\Pi}_{\perp n}$:

$$\boldsymbol{\Pi}_{\perp n} = \begin{pmatrix} \left(\frac{n\Omega_{\rm i}}{k_\perp}\right)^2 J_n^2(\mu) & \mathrm{i}v_\perp\frac{n\Omega_{\rm i}}{k_\perp}\,J_n(\mu)J_n'(\mu) \\ -\mathrm{i}v_\perp\frac{n\Omega_{\rm i}}{k_\perp}\,J_n(\mu)J_n'(\mu) & v_\perp^2\,\big(J_n'(\mu)\big)^2 \end{pmatrix}. \tag{11}$$

I employ the notation $J_n'(\mu) = \mathrm{d}J_n(\mu)/\mathrm{d}\mu$. The argument of the Bessel functions is $\mu \equiv k_\perp v_\perp/\Omega_{\rm i}$.

Let us denote the $2 \times 2$ matrix consisting of the ion susceptibilities $\chi_{xx}^{\rm i}$, $\chi_{yy}^{\rm i}$ and $\chi_{xy}^{\rm i} = -\chi_{yx}^{\rm i}$ by $\boldsymbol{\chi}_\perp^{\rm i}(\omega,\ \boldsymbol{k})$. Substituting the bi-Maxwellian (7) into (9) and performing the velocity integrations one finds after a significant amount of algebra:

$$\boldsymbol{\chi}_\perp^{\rm i}(\omega,\ \boldsymbol{k}) = \frac{\omega_{\rm pi}^2}{\omega^2}\sum_{n=-\infty}^{+\infty}\left[\frac{\omega}{\omega - n\Omega_{\rm i}}\,\{W(Z_n) - 1\} + \Delta_T\,W(Z_n)\right] \times \boldsymbol{\mathsf{M}}_{\perp n}. \tag{12}$$

Here $W(Z_n)$ is the plasma dispersion function defined by Ichimaru (1973, Ch.4):

$$W(Z_n) = \frac{1}{\sqrt{2\pi}} \int_{-\infty}^{+\infty} \mathrm{d}x \, \frac{x \exp(-x^2/2)}{x - Z_n}, \quad Z_n \equiv \frac{\omega - n\Omega_\mathrm{i}}{|k_\parallel| V_\parallel}. \tag{13}$$

It results from the integration over $v_\parallel$. The parameter $\Delta_T$ was defined in (8). The $2 \times 2$ tensor $\mathbf{M}_{\perp n}$ is obtained from the integration over $v_\perp$:

$$\mathbf{M}_{\perp n} = \begin{pmatrix} \dfrac{n^2}{\tilde{\mu}} \Lambda_n(\tilde{\mu}) & \mathrm{i}n \, \Lambda_n'(\tilde{\mu}) \\ -\mathrm{i}n \, \Lambda_n'(\tilde{\mu}) & \dfrac{n^2}{\tilde{\mu}} \Lambda_n(\tilde{\mu}) - 2\tilde{\mu} \, \Lambda_n'(\tilde{\mu}) \end{pmatrix}. \tag{14}$$

The function $\Lambda_n(\tilde{\mu})$ and its derivative $\Lambda_n'(\tilde{\mu}) \equiv \mathrm{d}\Lambda_n(\tilde{\mu})/\mathrm{d}\tilde{\mu}$ contain the finite gyration radius corrections. $\Lambda_n(\tilde{\mu})$ is given by

$$\Lambda_n(\tilde{\mu}) \equiv I_n(\tilde{\mu}) \exp(-\tilde{\mu}), \quad \tilde{\mu} = \frac{k_\perp^2 V_\perp^2}{\Omega_\mathrm{i}^2}, \tag{15}$$

with $I_n(\tilde{\mu})$ the modified Bessel function of the first kind. For the isotropic case, $\Delta_T = 0$, result (12) for $\boldsymbol{\chi}^\mathrm{i}_\perp(\omega, \boldsymbol{k})$ reduces to that of Ichimaru (1973, Ch. 5.2).

I know make the following two assumptions: [1] a *high-β plasma* with

$$\beta_\parallel = \frac{8\pi n_\mathrm{i} k_\mathrm{b} T_\parallel}{B_0^2} \gg 1, \quad \beta_\perp = \frac{8\pi n_\mathrm{i} k_\mathrm{b} T_\perp}{B_0^2} \gg 1, \tag{16}$$

and 2 *low-frequency, long wavelength waves* with (for positive $\omega$)

$$\omega \ll |k_\parallel| V_\parallel, \quad \omega \ll \Omega_\mathrm{i}, \quad \tilde{\mu} \ll 1. \tag{17}$$

In that case one has $|Z_0| \ll 1$ and one can use for $W(Z_0)$:

$$W(Z_0) \simeq 1 - Z_0^2 + \mathrm{i}\sqrt{\frac{\pi}{2}} \, Z_0 \exp\left(-Z_0^2/2\right). \tag{18}$$

In contrast, $|Z_n| \gg 1$ for $n = \pm 1, \pm 2, \ldots$ and $W(Z_n)$ satisfies

$$W(Z_n) \simeq -\frac{1}{Z_n^2} - \frac{3}{Z_n^4} \quad (\text{for } n \neq 0). \tag{19}$$

The imaginary term in the expression for $W(Z_0)$ comes from the Landau prescription for navigating the pole in the complex plane of the integral (13) at $x = Z_0$. It leads to the well-known effect of collisionless Landau damping of the wave modes at the Cerenkov resonance $\omega = k_\parallel v_\parallel$. As $|Z_n| \gg 1$ we can neglect the effect of cyclotron damping at the resonance $\omega = k_\parallel v_\parallel + n\Omega$ with $n \neq 0$.

The assumption $\tilde{\mu} \ll 1$ allows one to expand $\Lambda_n(\tilde{\mu})$ (e.g. Stix 1992, Ch. 10). Table 1 gives the result of this expansion for the elements of $\mathbf{M}_{\perp n}$ for $n = 0$, $\pm 1$ and $\pm 2$. I neglect terms of order $\tilde{\mu}^2$ and higher, which allows me to break off the summation over cyclotron harmonics (harmonic number $n$) after $n = \pm 2$.

At the same time we have to expand factors resulting involving $Z_n$ for $n = \pm 1, \pm 2$, for example:

$$\frac{1}{Z_1^2} = \frac{k_\parallel^2 V_\parallel^2}{(\omega - \Omega_\mathrm{i})^2} \simeq \frac{k_\parallel^2 V_\parallel^2}{\Omega_\mathrm{i}^2} \left(1 + 2\frac{\omega}{\Omega_\mathrm{i}} - 3\frac{\omega^2}{\Omega_\mathrm{i}^2} + \cdots\right). \tag{20}$$

**Table 1.** Components of $\mathbf{M}_{\perp n}$ for $\tilde{\mu} \ll 1$ to first order in $\tilde{\mu}$.

| Matrix element | $n = 0$ | $n = \pm 1$ | $n = \pm 2$ |
|---|---|---|---|
| $M_{xx}$ | 0 | $(1 - \tilde{\mu})/2$ | $\tilde{\mu}/2$ |
| $M_{yy}$ | $2\tilde{\mu}$ | $(1 - 3\tilde{\mu})/2$ | $\tilde{\mu}/2$ |
| $M_{xy} = -M_{yx}$ | 0 | $\pm\mathrm{i}(1 - 2\tilde{\mu})/2$ | $\pm\mathrm{i}\tilde{\mu}/2$ |

The second and third term inside the bracket terms give corrections that are usually neglected in the low-$\beta$ limit.

In order to make direct contact with the results obtained by Foote & Kulsrud (1979) for the isotropic case ($\Delta_T = 0$) I employ a similar set of dimensionless variables for parallel and perpendicular wavenumber and wave frequency. Dimensionless wavenumbers are defined in terms of $k_0 \equiv \Omega_\mathrm{i} V_\mathrm{A}/2V_\parallel^2$:

$$\ell_\parallel = \frac{k_\parallel}{k_0} = \frac{2k_\parallel V_\parallel^2}{\Omega_\mathrm{i} V_\mathrm{A}}, \quad \ell_\perp = \frac{T_\perp}{T_\parallel}\frac{k_\perp}{k_0} = \frac{2k_\perp V_\perp^2}{\Omega_\mathrm{i} V_\mathrm{A}}. \tag{21}$$

The dimensionless frequency is

$$\nu = \frac{\omega}{k_0 V_\mathrm{A}} = \frac{\omega\beta_\parallel}{\Omega_\mathrm{i}}. \tag{22}$$

Here $V_\mathrm{A}$ is the Alfvén speed defined in the usual manner, $V_\mathrm{A} = B_0/\sqrt{4\pi n_\mathrm{i} m_\mathrm{p}}$, neglecting the electron inertia. These definitions are based on the fact that wave properties in a high-$\beta$ plasma start to deviate significantly from the better-known cold plasma results for

$$k \sim k_0 = \frac{\Omega_\mathrm{i}}{V_\mathrm{A}\beta_\parallel}, \quad |\omega| \sim k_0 V_\mathrm{A} = \frac{\Omega_\mathrm{i}}{\beta_\parallel}, \tag{23}$$

that is at $(|\ell_\parallel|, \ell_\perp) \sim 1$ and $|\nu| \sim 1$.

A lengthy but relatively straightforward calculation gives the relevant components of the ion susceptibility tensor:

$$\begin{aligned}
\chi^\mathrm{i}_{xx} &= \frac{c^2}{V_\mathrm{A}^2} \left\{1 + \frac{3}{2}\frac{\ell_\parallel^2}{\beta_\parallel} - \frac{3}{8}\frac{\ell_\perp^2}{\beta_\perp} + \frac{\nu^2}{\beta_\parallel^2}\right\} \\
&\quad - \frac{c^2}{V_\mathrm{A}^2} \frac{\ell_\parallel^2 \beta_\parallel}{2\nu^2} \Delta_T \left\{1 + \frac{3}{2}\frac{\ell_\parallel^2}{\beta_\parallel} - \frac{3}{8}\frac{\ell_\perp^2}{\beta_\perp} + 3\frac{\nu^2}{\beta_\parallel^2}\right\}, \\
\chi^\mathrm{i}_{yy} &= \frac{c^2}{V_\mathrm{A}^2} \left\{1 + \frac{3}{2}\frac{\ell_\parallel^2}{\beta_\parallel} - \frac{11}{8}\frac{\ell_\perp^2}{\beta_\perp} + \frac{\nu^2}{\beta_\parallel^2}\right\} \\
&\quad - \frac{c^2}{V_\mathrm{A}^2} \frac{\ell_\parallel^2 \beta_\parallel}{2\nu^2} \Delta_T \left\{1 + \frac{3}{2}\frac{\ell_\parallel^2}{\beta_\parallel} - \frac{3}{8}\frac{\ell_\perp^2}{\beta_\perp} + 3\frac{\nu^2}{\beta_\parallel^2}\right\} \\
&\quad + \frac{c^2}{V_\mathrm{A}^2} \frac{\ell_\perp^2}{\nu^2} \left\{\mathrm{i}\sqrt{\pi} \frac{\beta_\parallel^{1/2} \nu}{|\ell_\parallel|} \exp\left(-\frac{\nu^2}{\beta_\parallel \ell_\parallel^2}\right) \right. \\
&\quad \left. - \frac{2\nu^2}{\ell_\parallel^2} + \left(\frac{\beta_\parallel^2}{\beta_\perp}\right) \Delta_T \right\}, \\
\chi^\mathrm{i}_{xy} &= -\chi^\mathrm{i}_{yx} = \mathrm{i}\frac{c^2}{V_\mathrm{A}^2}\frac{\beta_\parallel}{\nu} \left\{1 + \frac{1}{2}\frac{\ell_\parallel^2}{\beta_\parallel} - \frac{3}{4}\frac{\ell_\perp^2}{\beta_\perp} + \frac{\nu^2}{\beta_\parallel^2}\right\} \\
&\quad - \mathrm{i}\frac{c^2}{V_\mathrm{A}^2}\frac{\ell_\parallel^2}{\nu} \Delta_T \left\{1 + 3\frac{\ell_\parallel^2}{\beta_\parallel} - \frac{15}{16}\frac{\ell_\perp^2}{\beta_\perp} + 2\frac{\nu^2}{\beta_\parallel^2}\right\}.
\end{aligned} \tag{24}$$

Here I have used $\beta_\parallel = 2V_\parallel^2/V_\mathrm{A}^2$ and $\beta_\perp = 2V_\perp^2/V_\mathrm{A}^2$. Since only a small anisotropy is needed ($|\Delta_T| \sim 1/\beta$) for the firehose- and mirror instabilities discussed below, the term $\propto \Delta_T$ in the expression for $\chi^\mathrm{i}_{xy}$ can be simplified: the factor in curly brackets may be approximated by unity as the finite Larmor radius corrections then correspond to a set terms of order $1/\beta^2$. Terms of similar magnitude are also neglected in the rest of the expression.

### 2.2 Electron response

The electron contribution to the plasma susceptibility can be calculated in the same manner, using the electron version of relation (9).

There are, however, a number of significant simplifications that result from the assumptions. We neglect the electron temperature anisotropy as we expect $\Delta_T^{\rm e} \sim \left(m_{\rm e}/m_{\rm p}\right)^{1/2}\ \Delta_T \sim 0.025\Delta_T$ to be very small. This is due to the fact that electron–electron collisions that tend to erase electron pressure anisotropies are a factor $\sqrt{m_{\rm p}/m_{\rm e}}$ more frequent than the ion–ion collisions that do the same for the ions. In what follows will put $\Delta_T^{\rm e} = 0$. In addition, the finite gyration radius corrections are very small: $\tilde{\mu}^{\rm e} \sim \left(m_{\rm e}/m_{\rm p}\right)\tilde{\mu} \simeq 0.0005\,\tilde{\mu}$. That means that we can use the leading terms in the expansion of the components of $\mathbf{M}^{\rm e}_{\perp n}$, the electron version of Table 1. Unless the electrons are significantly hotter than the ions,

$$T_{\rm e} > \left(m_{\rm p}/m_{\rm e}\right)^{1/2}\ T_{\rm i}, \tag{25}$$

this implies that the only the $n = 0, \pm 1$ terms need to be taken into account, with $M_{yy}(0) \simeq 2\tilde{\mu}_{\rm e}$, $M^{\rm e}_{xx}(\pm1) = M^{\rm e}_{yy}(\pm1) \simeq 1/2$ and $M^{\rm e}_{xy}(\pm1) = -M^{\rm e}_{yx}(\pm1) \simeq \pm{\rm i}/2$, with $\tilde{\mu}_{\rm e} \equiv k_\perp^2 V_{\rm e}^2/\Omega_{\rm e}^2$ (compare Table 1). Here I introduce the electron thermal velocity

$$V_{\rm e} = \sqrt{k_{\rm b}T_{\rm e}/m_{\rm e}}. \tag{26}$$

I *will* allow for an electron current along the magnetic field, adopting a drifting Maxwellian distribution for the electrons, $\mathrm{d}n_{\rm e} = n_{\rm e}\, f_{\rm e}(v_\perp,\ v_\parallel)\, 2\pi v_\perp \mathrm{d}v_\perp\, \mathrm{d}v_\parallel$ with

$$f_{\rm e}(v_\perp,\ v_\parallel) = \frac{1}{(2\pi V_{\rm e}^2)^{3/2}} \exp\left(-\frac{v_\perp^2 + (v_\parallel - U)^2}{2V_{\rm e}^2}\right). \tag{27}$$

Here $U$ is the electron drift velocity ($\langle v_\parallel\rangle = U$) with respect to the ions. Since the elements of the $2\times 2$ matrix $\mathbf{\Pi}_{\perp n}$ do not *explicitly* involve $v_\parallel$, the drift leads to the replacement of the wave frequency $\omega$ by its Doppler-shifted version,[1]

$$\omega \implies \tilde{\omega} = \omega - k_\parallel U. \tag{28}$$

This is easily seen from using the drifting the Maxwellian distribution function $f_{\rm e}(v_\perp, v_\parallel)$ together with a simple change of integration variable from $v_\parallel$ to $\tilde{v}_\parallel \equiv v_\parallel - U$ in the integration over $v_\parallel$. The electron susceptibility $\boldsymbol{\chi}^{\rm e}_\perp$ is formally

$$\boldsymbol{\chi}^{\rm e}_\perp(\omega,\ \boldsymbol{k}) = \frac{\omega_{\rm pe}^2}{\omega^2}\sum_{n=-\infty}^{+\infty}\left[\frac{\tilde{\omega}}{\tilde{\omega} - n\Omega_{\rm e}}\left\{W(\tilde{Z}_n) - 1\right\}\right]\mathbf{M}_{\perp n}. \tag{29}$$

Here $\omega_{\rm pe} = \sqrt{4\pi e^2 n_{\rm e}/m_{\rm e}}$ is the electron plasma frequency and

$$\tilde{Z}_n \equiv \frac{\tilde{\omega} - n\Omega_{\rm e}}{|k_\parallel| V_{\rm e}} = \frac{\omega - k_\parallel U - n\Omega_{\rm e}}{|k_\parallel| V_{\rm e}}, \quad \Omega_{\rm e} = -\frac{eB_0}{m_{\rm e}c} = -|\Omega_{\rm e}|. \tag{30}$$

Assuming $T_{\rm e}$ to be similar to the ion temperatures $T_\parallel$ and $T_\perp$ and consistently neglecting terms of order $\sqrt{m_{\rm e}/m_{\rm p}}, m_{\rm e}/m_{\rm p}$ with respect to unity one finds (using the above considerations) that the electron susceptibility becomes very simple:

$$\chi^{\rm e}_{xx} \simeq \frac{\omega_{\rm pe}^2}{\Omega_{\rm e}^2}\frac{\tilde{\omega}^2}{\omega^2} = \frac{m_{\rm e}}{m_{\rm p}}\frac{c^2}{V_{\rm A}^2}\frac{\tilde{\omega}^2}{\omega^2},$$

$$\chi^{\rm e}_{yy} \simeq \frac{\omega_{\rm pe}^2}{\Omega_{\rm e}^2}\frac{\tilde{\omega}^2}{\omega^2} + \sqrt{2\pi}\,{\rm i}\,\frac{\omega_{\rm pe}^2}{\Omega_{\rm e}^2}\frac{k_\perp^2 V_{\rm e}^2}{\omega^2}\frac{\tilde{\omega}}{|k_\parallel| V_{\rm e}}\exp\left(-\frac{\tilde{\omega}^2}{k_\parallel^2 V_{\rm e}^2}\right),$$

$$\chi^{\rm e}_{xy} = -\chi^{\rm e}_{yx} \simeq -{\rm i}\,\frac{\omega_{\rm pe}^2}{\omega^2|\Omega_{\rm e}|}\tilde{\omega}. \tag{31}$$

Using $V_{\rm e} \simeq \sqrt{m_{\rm p}/m_{\rm e}}\,V_\parallel$, $\omega_{\rm pe} = \sqrt{m_{\rm p}/m_{\rm e}}\,\omega_{\rm pi}$ and $|\Omega_{\rm e}| = (m_{\rm p}/m_{\rm e})\,\Omega_{\rm i}$ it is easily checked that the electron contribution to the $xx$ and $yy$ components of $\boldsymbol{\chi}_\perp$ can be neglected altogether with respect to the ion terms unless the drift velocity becomes very large (i.e. $U > (m_{\rm p}/m_{\rm e})^{1/2}\,|\omega/k_\parallel|$). In practice, there are other plasma instabilities (in particular, electrostatic two-stream instabilities) that prevent this from happening. However, the $xy$ component of $\boldsymbol{\chi}^{\rm e}_\perp$ is important. It can be written as

$$\chi^{\rm e}_{xy} = -{\rm i}\,\frac{c^2}{V_{\rm A}^2}\frac{\beta_\parallel}{\nu}\frac{n_{\rm e}}{n_{\rm i}}\left(1 - \frac{k_\parallel U}{\omega}\right). \tag{32}$$

If there is no electron current with respect to the ions ($U = 0$) and no net charge density (so that $n_{\rm e} = n_{\rm i}$), this term exactly cancels the corresponding (leading) term in the ion susceptibility $\chi^{\rm i}_{xy}$. This is the near-cancellation of the electron- and ion currents associated with the $\boldsymbol{E}\ \times \boldsymbol{B}_0$ drift that was referred to in the Introduction.

### 2.3 Total response for a simple two-temperature plasma

For a simple quasi-neutral plasma ($n_{\rm e} = n_{\rm i}$) without electron current ($U = 0$) the total susceptibility is the sum of the ion and electron susceptibilities. As argued above, the $xx$ and $yy$ components of $\boldsymbol{\chi}_\perp(\omega,\ \boldsymbol{k})$ are adequately described by the ion terms alone, given in equation (24). The off-diagonal components satisfy

$$\chi_{xy} = -\chi_{yx} = {\rm i}\,\frac{c^2}{V_{\rm A}^2}\left\{\frac{1}{2}\frac{\ell_\parallel^2}{\nu} - \frac{3}{4}\frac{\beta_\parallel\ell_\perp^2}{\beta_\perp\nu} + \frac{\nu}{\beta_\parallel}\right\} - {\rm i}\,\frac{c^2}{V_{\rm A}^2}\frac{\ell_\parallel^2}{\nu}\,\Delta_T. \tag{33}$$

In what follows I use the dimensionless phase speed $\upsilon$, defined as

$$\upsilon \equiv \frac{\omega}{|k_\parallel| V_{\rm A}} = \frac{\nu}{|\ell_\parallel|}, \tag{34}$$

the wave frequency in units of the frequency of the classical Alfvén wave. I also assume a non-relativistic plasma in the sense that $V_{\rm A}^2/c^2 \ll 1$. Finally, it is useful to define the quantity

$$Q \equiv 1 + \frac{3}{2}\frac{\ell_\parallel^2}{\beta_\parallel} - \frac{3}{8}\frac{\ell_\perp^2}{\beta_\perp}. \tag{35}$$

In most cases we can use $Q \simeq 1$. With these definitions dispersion relation (6) in dimensionless variables can be written as

$$\left\{\frac{\ell_\parallel^2}{\beta_\parallel^2}\,\upsilon^4 + Q\,\upsilon^2 - \mathcal{F}(\beta_\perp,\ \beta_\parallel)\right\}$$

$$\times\left\{\frac{\ell_\parallel^2}{\beta_\parallel^2}\,\upsilon^4 + Q\,\upsilon^2 - \mathcal{F}(\beta_\perp,\ \beta_\parallel) - \left(\frac{\ell_\perp}{\ell_\parallel}\right)^2\left[\left(\frac{T_\parallel}{T_\perp}\right)^2\mathcal{M}(\beta_\perp,\ \beta_\parallel)\right.\right.$$

$$\left.\left. + \frac{\ell_\parallel^2}{\beta_\perp}\,\upsilon^2 + 2\upsilon^2 - {\rm i}\sqrt{\pi\beta_\parallel}\,\upsilon\exp\left(-\upsilon^2/2\beta_\parallel\right)\right]\right\}$$

$$-\frac{\ell_\parallel^2\upsilon^2}{4}\left\{1 - \frac{3}{2}\left(\frac{\beta_\parallel}{\beta_\perp}\right)\left(\frac{\ell_\perp}{\ell_\parallel}\right)^2 + 2\frac{\upsilon^2}{\beta_\parallel} - 2\Delta_T\right\}^2 = 0. \tag{36}$$

The effects of the ion temperature anisotropy are represented in (36) by the *firehose function*,

$$\mathcal{F}(\beta_\perp,\ \beta_\parallel) \equiv 1 + \frac{\beta_\parallel Q\Delta_T}{2} \simeq 1 + \frac{\beta_\perp - \beta_\parallel}{2}, \tag{37}$$

[1] It is perhaps good to point out that a similar line of reasoning does not hold for the components of the full susceptibility tensor $\boldsymbol{\chi}^{\rm e}$ (and the corresponding components of $\mathbf{\Pi}$) that are not considered here, such as $\chi_{xz}$ or $\chi_{zz}$. These components of $\mathbf{\Pi}_n$ do depend explicitly on $v_\parallel$ and a non-vanishing $\langle v_\parallel\rangle$ leads to additional terms in addition to the replacement $\omega \implies \tilde{\omega}$.

and the *mirror function*,

$$\mathcal{M}(\beta_\perp,\ \beta_\parallel) \equiv 1 - \beta_\perp\ \Delta_T = 1 - \frac{\beta_\perp}{\beta_\parallel}\ \left(\beta_\perp - \beta_\parallel\right). \tag{38}$$

Here $\beta_\perp$ and $\beta_\parallel$ refer to ion pressure alone. The approximate equality in (37) is valid if $\ell_\parallel^2/\beta_\parallel \ll 1$, $\ell_\perp^2/\beta_\perp \ll 1$ so that $Q \simeq 1$. These two terms are responsible for the firehose instability and the mirror instability. In the classical (low-$\beta$) case they occur, respectively, when $\mathcal{F}(\beta_\perp,\ \beta_\parallel) < 0$ when $k \sim |k_\parallel|$ and $\mathcal{M}(\beta_\perp,\ \beta_\parallel) < 0$ when $k \sim k_\perp$. In the rest of this paper I will refer to instabilities occurring when $\Delta_T < 0$ as firehose instabilities, and those that occur for $\Delta_T > 0$ as mirror instabilities

If there is no temperature anisotropy ($\Delta_T = 0$, $\mathcal{F} = \mathcal{M} = 1$) dispersion relation (36) reduces to the result of Foote & Kulsrud (1979), their equations (9)–(11). They employ slightly different variables and one needs the substitutions $\ell_\parallel \Longrightarrow \ell$ and $\ell_\parallel \Longrightarrow \ell\ \tan\theta$ (where $\theta$ is the angle between $\boldsymbol{B}_0$ and $\boldsymbol{k}$) to get complete correspondence with their expressions.

## 3 PARALLEL PROPAGATION: THE FIREHOSE INSTABILITY

It is instructive to see to what extent the well-known result for the firehose instability is changed in a high-$\beta$ plasma. The firehose instability is associated with waves that propagate quasi-parallel to the magnetic field, that is for wavenumbers satisfying

$$\left|\frac{k_\perp}{k_\parallel}\right| = \left(\frac{T_\parallel}{T_\perp}\right)\ \left|\frac{\ell_\perp}{\ell_\parallel}\right| \ll 1. \tag{39}$$

If we assume $\ell_\parallel^2/\beta_\perp \ll 1$ we can put $Q = 1$ and dispersion relation (36) may be approximated by

$$\left(\upsilon^2 - \mathcal{F}(\beta_\perp,\ \beta_\parallel)\right)^2 - \frac{\ell_\parallel^2\upsilon^2}{4} = 0. \tag{40}$$

We can neglect the Landau damping term for these modes. It will be considered in the next section. The four solutions to this bi-quadratic dispersion relation for $\upsilon$ come in the form of $\upsilon_+, -\upsilon_+, \upsilon_-, -\upsilon_-$, with $\upsilon_\pm$, defined as

$$\upsilon_\pm \equiv \sqrt{\mathcal{F}(\beta_\perp,\ \beta_\parallel) + \frac{\ell_\parallel^2}{16}} \pm \frac{|\ell_\parallel|}{4}. \tag{41}$$

In a plasma without an (ion) temperature anisotropy ($\beta_\parallel = \beta_\perp$ so that $\mathcal{F}(\beta_\perp,\ \beta_\parallel) = 1$), this relation reduces to the one derived by Foote & Kulsrud (1979), their equation (18). The cold plasma limit corresponds to $|\ell_\parallel| \downarrow 0$, and one recovers the well-known firehose dispersion relation, in physical variables

$$\omega^2 = k_\parallel^2 V_\mathrm{A}^2\ \left(1 + \frac{\beta_\perp - \beta_\parallel}{2}\right). \tag{42}$$

Unstable solutions with $\mathrm{Im}(\omega) > 0$ are possible if the argument of the square root in (41) becomes negative, which occurs when $\mathcal{F}(\beta_\perp,\ \beta_\parallel) + \ell_\parallel^2/16 < 0$, in physical variables

$$\left(1 - \frac{k_\parallel^2 V_\parallel^2}{4\,\Omega_\mathrm{i}^2}\right) P_\parallel > P_\perp + \frac{B_0^2}{4\pi}. \tag{43}$$

This shows that the inclusion of finite-$\beta$ effects (ion velocity dispersion along the field) has a stabilizing influence: a larger pressure anisotropy is needed for unstable behaviour at shorter wavelengths as $|\ell_\parallel|$ increases. In addition, the frequency of the unstable mode is complex, rather than purely imaginary as in the cold plasma case, due to the dispersion introduced by the $\ell_\parallel^2$ term. The unstable wavenumbers are in the range

$$0 \le |\ell_\parallel| < \ell_\mathrm{m} \equiv 4\sqrt{|\mathcal{F}(\beta_\perp,\ \beta_\parallel)|}. \tag{44}$$

The maximum growth rate occurs at $|\ell_\parallel| = \ell_\mathrm{m}/\sqrt{2} \equiv \ell_*$. The maximum growth rate (in units of $k_0 V_\mathrm{A}$) is

$$\sigma_\mathrm{max} = \frac{\mathrm{Im}(\nu)_\mathrm{max}}{k_0 V_\mathrm{A}} = \frac{\ell_*}{\sqrt{2}}\ \sqrt{|\mathcal{F}(\beta_\perp,\ \beta_\parallel)|} = 2\,|\mathcal{F}(\beta_\perp,\ \beta_\parallel)|. \tag{45}$$

To summarize: the term $\propto k_\parallel^2 V_\parallel^2/\Omega_\mathrm{i}^2$ in the dispersion relation regularizes the behaviour of the firehose instability at short wavelengths, and introduces a maximum growth rate at $|k_\parallel| = \sqrt{2|\mathcal{F}|}\,(\Omega_\mathrm{i} V_\mathrm{A}/V_\parallel^2)$.

One can find useful approximations to relation (41) in the two limits $\ell_\parallel^2/16 \ll |\mathcal{F}(\beta_\perp,\ \beta_\parallel)|$ and $|\mathcal{F}(\beta_\perp,\ \beta_\parallel)| \ll \ell_\parallel^2 \ll 2\beta_\parallel$. In the first case one finds

$$\upsilon_\pm = \sqrt{\mathcal{F}(\beta_\perp,\ \beta_\parallel)} \pm \frac{|\ell_\parallel|}{4} = \sqrt{1 + \frac{\beta_\perp - \beta_\parallel}{2}} \pm \frac{|\ell_\parallel|}{4}, \tag{46}$$

or equivalently in physical variables

$$\omega_\pm = |k_\parallel| V_\mathrm{A}\ \sqrt{1 + \frac{\beta_\perp - \beta_\parallel}{2}} \pm \frac{k_\parallel^2 V_\parallel^2}{2\Omega_\mathrm{i}}. \tag{47}$$

Both modes are unstable if the classical firehose criterion

$$P_\parallel > P_\perp + \frac{B_0^2}{4\pi} \tag{48}$$

is satisfied.

In the limit $|\mathcal{F}(\beta_\perp,\ \beta_\parallel)| \ll \ell_\parallel^2 \ll 2\beta_\parallel$ one gets a large ($\upsilon_+ \gg 1$) and a small ($\upsilon_- \ll 1$) solution, respectively, given by

$$\upsilon_+ \simeq \frac{|\ell_\parallel|}{2} + \frac{2 + \beta_\perp - \beta_\parallel}{|\ell_\parallel|} \tag{49}$$

and

$$\upsilon_- \simeq \left(1 + \frac{\beta_\perp - \beta_\parallel}{2}\right)\ \frac{2}{|\ell_\parallel|}. \tag{50}$$

Taking only the leading terms, these two solutions correspond in physical variables to

$$\omega_+ \simeq \frac{k_\parallel^2 V_\parallel^2}{\Omega_\mathrm{i}} = \frac{\beta_\parallel}{2}\ \frac{k_\parallel^2 V_\mathrm{A}^2}{\Omega_\mathrm{i}}, \quad \omega_- \simeq \left(1 + \frac{\beta_\perp - \beta_\parallel}{2}\right)\ \frac{2\Omega_\mathrm{i}}{\beta_\parallel}. \tag{51}$$

These short-wavelength modes are stable, in accordance with the discussion above.

Fig. 1 shows the solution of the dispersion relation for the case of an isotropic plasma ($\mathcal{F}(\beta_\perp,\ \beta_\parallel) = 1$). Fig. 2 shows the firehose-unstable case $\mathcal{F}(\beta_\perp,\ \beta_\parallel) = -1$. This last figure is representative for all cases with $\mathcal{F}(\beta_\perp,\ \beta_\parallel) < 0$.

## 4 OBLIQUE PROPAGATION: FIREHOSE/MIRROR INSTABILITIES

When $k_\perp \neq 0$, but $k_\perp$ is still small compared with $k_\parallel$, new wave modes become possible as the Landau term $\propto \mathrm{i}\sqrt{\pi\beta_\parallel}$ in $\chi_{yy}$ becomes important. Its importance can be represented by the parameter $\alpha$ (following Foote & Kulsrud 1979, who employ instead $\alpha_\mathrm{FK} = \ell_\parallel^2\,\alpha$) defined as

$$\alpha \equiv \sqrt{\pi\beta_\parallel}\ \left(\frac{\ell_\perp}{\ell_\parallel}\right)^2. \tag{52}$$

Note that $\alpha \sim 1$ when $k_\perp \sim k_\parallel/(\pi\beta_\parallel)^{1/4} \ll k_\parallel$ if $\beta_\parallel$ is sufficiently large.

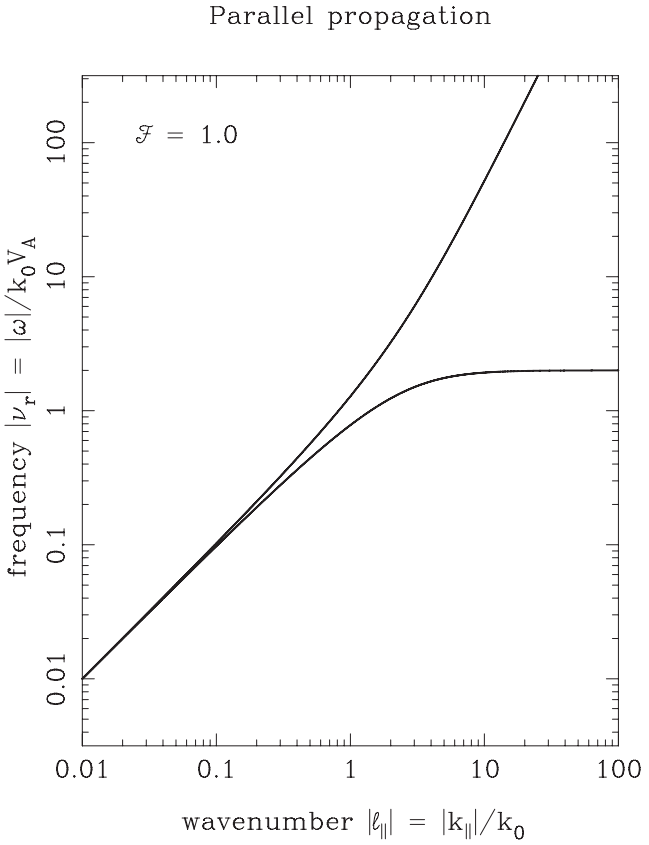


**Figure 1.** The two solutions to the dispersion relation for pure parallel propagation ($\ell_\perp = 0$) in an isotropic plasma with $T_\parallel = T_\perp$.

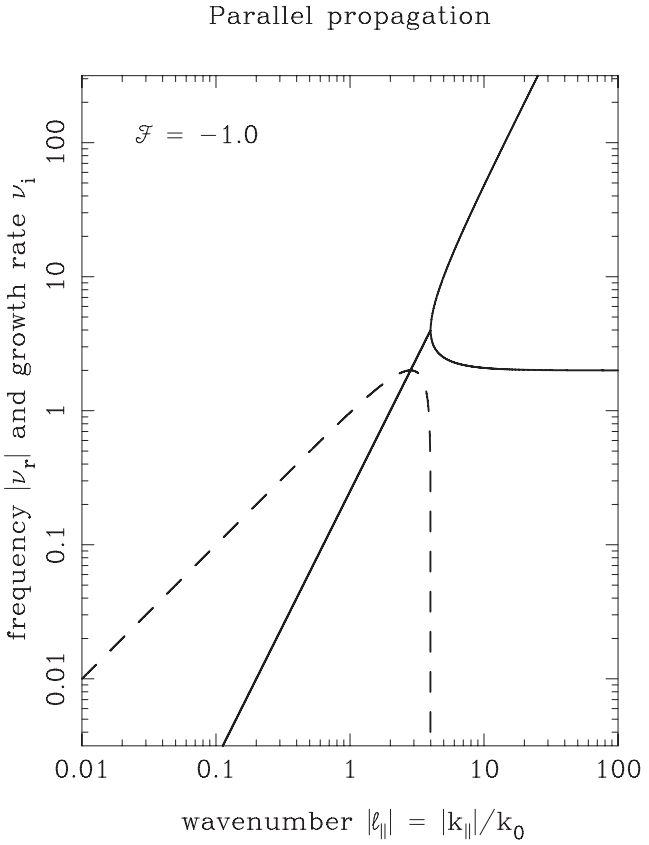


**Figure 2.** The solutions to the dispersion relation for pure parallel propagation ($\ell_\perp = 0$) in the firehose-unstable case with $\mathcal{F}(\beta_\perp,\ \beta_\parallel) = -1$. The solid curves give the real part of the dimensionless frequency, $\nu = \nu_r + i\nu_i$, and the dashed curve gives the growth rate $\nu_i$. Wave growth occurs for $|\ell_\parallel| < \ell_m = 4\sqrt{|\mathcal{F}|} = 4$. For $|\ell_\parallel| < \ell_m$ there is one growing mode and a corresponding decaying mode, both with same $\nu_r$. For $|\ell_\parallel| > \ell_m$ there are two modes (a low- and a high-frequency mode) with a purely real frequency ($\nu_i = 0$).

For low-frequency waves with $|\upsilon| \ll \sqrt{2\beta_\parallel}$ one can put $\exp(-\upsilon^2/2\beta_\parallel) \simeq 1$, use $Q \simeq 1$ and neglect all terms involving $\ell_\parallel^2\upsilon^4/\beta_\parallel^2$ in (36), as well as the terms $\propto \upsilon^2$ inside the square brackets in the second factor of the first term of (36). The dispersion relation simplifies considerably:

$$\left(\upsilon^2 - \mathcal{F}(\beta_\perp,\ \beta_\parallel)\right)\ \left(\upsilon^2 + i\alpha\,\upsilon - \mathcal{G}(\beta_\perp,\ \beta_\parallel)\right) - \frac{\ell_\parallel^2\upsilon^2}{4} = 0. \quad (53)$$

Here I define

$$\mathcal{G}(\beta_\perp,\ \beta_\parallel) \equiv \mathcal{F}(\beta_\perp,\ \beta_\parallel) + \left(\frac{k_\perp}{k_\parallel}\right)^2\ \mathcal{M}(\beta_\perp,\ \beta_\parallel)$$

$$= \mathcal{F}(\beta_\perp,\ \beta_\parallel) + \left(\frac{T_\perp}{T_\parallel}\right)^2\ \frac{\alpha\,\mathcal{M}(\beta_\perp,\ \beta_\parallel)}{\sqrt{\pi\beta_\parallel}}. \quad (54)$$

Note that $\mathcal{G}(\beta_\perp,\ \beta_\parallel) = \mathcal{F}(\beta_\perp,\ \beta_\parallel)$ for $\alpha = 0$ (parallel propagation). In that case this dispersion relation reverts to relation (40) and the results of Section 3 apply.

An alternative form of dispersion relation (53) proves useful. Defining

$$\xi_\pm \equiv \frac{i\alpha}{2} \pm \frac{\sqrt{\ell_\parallel^2 - \alpha^2}}{2}, \quad (55)$$

one can rewrite (53) as

$$\left(\upsilon^2 + \xi_-\,\upsilon - \mathcal{F}(\beta_\perp,\ \beta_\parallel)\right)\left(\upsilon^2 + \xi_+\,\upsilon - \mathcal{G}(\beta_\perp,\ \beta_\parallel)\right)$$

$$+ \xi_-\upsilon\ \left(\mathcal{G}(\beta_\perp,\ \beta_\parallel) - \mathcal{F}(\beta_\perp,\ \beta_\parallel)\right) = 0. \quad (56)$$

I will consider the solutions of (53/56) in various limits.

### 4.1 Case $\alpha \le |\ell_\parallel|$ and $|\ell_\parallel| \ll 1$

In this case $|\xi_-| \sim |\xi_+| \sim \alpha \ll 1$ and $|\mathcal{G} - \mathcal{F}| \sim \alpha/\sqrt{\pi\beta_\parallel} \ll 1$. Then (56) is the best approximation for the dispersion relation, where one can neglect the last term on the left-hand side, which is formally of order $\alpha^2/\sqrt{\pi\beta_\parallel} \ll \alpha^2$. The solutions are

$$\upsilon = -\frac{\xi_+}{2} \pm \sqrt{\mathcal{G} + \frac{\xi_+^2}{4}} \quad (57)$$

and

$$\upsilon = -\frac{\xi_-}{2} \pm \sqrt{\mathcal{F} + \frac{\xi_-^2}{4}}. \quad (58)$$

If $\alpha \ll |\ell_\parallel|$ we can put

$$\xi_\pm \simeq \pm\frac{|\ell_\parallel|}{2} + \frac{i\alpha}{2},\ \ \xi_\pm^2 \simeq \frac{\ell_\parallel^2}{4} \pm \frac{i\alpha\,|\ell_\parallel|}{2} + \mathcal{O}(\alpha^2). \quad (59)$$

We get the solutions (leaving the complex roots unresolved)

$$\upsilon = -\frac{|\ell_\parallel|}{4} - \frac{i\alpha}{4} \pm \sqrt{\mathcal{G} + \frac{\ell_\parallel^2}{16} + \frac{i\alpha\,|\ell_\parallel|}{8}} \quad (60)$$

and

$$\upsilon = +\frac{|\ell_\parallel|}{4} - \frac{\mathrm{i}\alpha}{4} \pm \sqrt{\mathcal{F} + \frac{\ell_\parallel^2}{16} - \frac{i\alpha\,|\ell_\parallel|}{8}}. \tag{61}$$

This is a minor modification of the parallel modes discussed in Section 3 as $|\mathcal{G} - \mathcal{F}| = \mathcal{O}(\alpha)$. The term $-\mathrm{i}\alpha/4$ represents Landau damping.

### 4.2 Case $\alpha \simeq 1$ and $|\ell_\parallel| \ll 1$

Here we can again employ form (56) of the dispersion relation together with

$$\xi_+ \simeq \mathrm{i}\alpha\ , \quad \xi_- \simeq \frac{\mathrm{i}\ell_\parallel^2}{4\alpha} \ll 1. \tag{62}$$

As $|\xi_-| \ll |\xi_+|$ we can again neglect the last term on the left-hand side of (56). Then the formal solutions are

$$\upsilon = -\frac{\mathrm{i}\alpha}{2} \pm \sqrt{\mathcal{G} - \frac{\alpha^2}{4}} \tag{63}$$

and

$$\upsilon = -\frac{\mathrm{i}\ell_\parallel^2}{8\alpha} \pm \sqrt{\mathcal{F} - \frac{\ell_\parallel^4}{64\alpha^2}}. \tag{64}$$

Respectively these two solutions correspond to a 'large' ($|\upsilon| \sim \alpha \sim 1$) and a 'small' ($|\upsilon| \sim \ell_\parallel^2/\alpha \ll 1$) solution. The large solution can also be obtained from (53) by neglecting the coupling term.

The instability conditions are, respectively, $\mathcal{G} < 0$ (mirror instability) and $\mathcal{F} < 0$ (firehose instability). The condition $\mathcal{G} < 0$ can be written in terms of physical variables as

$$k_\parallel^2 \left(\frac{B_0^2}{4\pi} + P_\perp - P_\parallel\right) + 2k_\perp^2 \left(\frac{B_0^2}{8\pi} - P_\perp \left[\frac{T_\perp}{T_\parallel} - 1\right]\right) < 0, \tag{65}$$

the classical condition for the firehose instability that is also found in the low-$\beta$ case. For small anisotropies (with $\beta_\parallel \simeq \beta_\perp \equiv \beta$ and $\Delta_T \ll 1$) condition (65) can be approximated as

$$k^2 - \beta\,\Delta_T \left(k_\perp^2 - \frac{k_\parallel^2}{2}\right) < 0. \tag{66}$$

Modes with $k_\perp < k_\parallel/\sqrt{2}$ are potentially firehose unstable if $\Delta_T$ is negative ($P_\parallel > P_\perp$). Modes with $k_\perp > k_\parallel/\sqrt{2}$ can be mirror-unstable if $\Delta_T$ is positive ($P_\perp > P_\parallel$). This agrees with the conclusions of Schekochihin et al. (2005), see also Schekochihin et al. (2010). Close to the mirror instability boundary $\mathcal{G} = 0$ one can expand the square root in (63) for $|\mathcal{G}| \ll \alpha^2/4$ and get

$$\upsilon \simeq -\frac{\mathrm{i}\mathcal{G}}{\alpha}. \tag{67}$$

In physical variables this is

$$\omega = -\mathrm{i}|k_\parallel|V_\parallel \sqrt{\frac{2}{\pi}} \left(\frac{\beta_\parallel}{\beta_\perp^2}\right) \left\{ \left(\frac{k_\parallel}{k_\perp}\right)^2 \left(1 + \frac{\beta_\perp - \beta_\parallel}{2}\right) + \left[1 + \beta_\perp \left(\frac{\beta_\perp}{\beta_\parallel} - 1\right)\right] \right\}. \tag{68}$$

This low-frequency/long wavelength solution coincides with the one found in the low-$\beta$ case (e.g. Hasegawa 1975; Southwood & Kivelson 1993) using similar assumptions. In this limit finite Larmor radius effects can be entirely neglected.

### 4.3 Case $\alpha \sim |\ell_\parallel| \gg 1$

Here we have *large solutions* with $|\upsilon| \sim \alpha$. As long as $|\mathcal{F}|,\ |\mathcal{G}| \ll \alpha$ we can neglect the $\mathcal{F}$ and $\mathcal{G}$ terms (56), leading to

$$\upsilon = -\xi_+ = -\frac{\mathrm{i}\alpha}{2} - \frac{\sqrt{\ell_\parallel^2 - \alpha^2}}{2} \tag{69}$$

and

$$\upsilon = -\xi_- = -\frac{\mathrm{i}\alpha}{2} + \frac{\sqrt{\ell_\parallel^2 - \alpha^2}}{2}. \tag{70}$$

These modes are always damped. In addition there are *small solutions* with $|\upsilon| \sim 1/\alpha \ll 1$. These solutions can be obtained by neglecting the $\upsilon^4$ and $\upsilon^3$ terms in (53), and assuming $\ell_\parallel^2/4 \gg |\mathcal{F}|,\ |\mathcal{G}|$. The approximate dispersion relation becomes

$$\frac{\ell_\parallel^2}{4}\,\upsilon^2 + \mathrm{i}\alpha\,\mathcal{F}\,\upsilon - \mathcal{F}\mathcal{G} = 0. \tag{71}$$

The solution reads, using (54) for $\mathcal{G}$:

$$\upsilon = -\frac{2\mathrm{i}\alpha\mathcal{F}}{\ell_\parallel^2} \pm \frac{2}{\ell_\parallel^2}\sqrt{\ell_\parallel^2\,\mathcal{F}\mathcal{G} - \alpha^2\mathcal{F}^2}$$

$$= -\frac{2\mathrm{i}\alpha\mathcal{F}}{\ell_\parallel^2} \pm \frac{2}{\ell_\parallel^2}\sqrt{\left(\ell_\parallel^2 - \alpha^2\right)\mathcal{F}^2 + \ell_\perp^2 \left(\frac{T_\perp}{T_\parallel}\right)^2 \mathcal{M}}. \tag{72}$$

There is a firehose-unstable mode (with $\mathrm{Im}(\upsilon) > 0$) for both signs in front of the square root when $\mathcal{F} < 0$ (which implies $\mathcal{M} > 1 + 2(\beta_\perp/\beta_\parallel) \simeq 3$). If $\mathcal{F} > 0$ and $\mathcal{G} < 0$ (which requires $\mathcal{M} < 0$) there is a mirror-unstable mode. In the limit $|\mathcal{G}| \ll (\alpha/\ell_\parallel)^2\,\mathcal{F}$ the unstable solution occurs in the mode with the plus sign in front of the root, and its growth rate is again given by (67). The other mode is damped.

### 4.4 Case $\alpha \sim \ell_\parallel^2$ and $|\ell_\parallel| \gg 1$

Again we can use (62) and employ form (56) of the dispersion relation. Here there are three relevant solution families.

#### *4.4.1 Large solution*

For $|\upsilon| \sim \alpha \gg |\mathcal{F}|, |\mathcal{G}|$ we can neglect the $\mathcal{F}$ and $\mathcal{G}$ terms in the dispersion relation and one again finds solution (69). As $\alpha^2 \sim \ell_\parallel^4 \gg \ell_\parallel^2$ it can be written as

$$\upsilon \simeq -\xi_+ = -\frac{\mathrm{i}\alpha}{2}\left(1 + \sqrt{1 - \frac{\ell_\parallel^2}{\alpha^2}}\right) \simeq -\mathrm{i}\alpha\left(1 - \frac{\ell_\parallel^2}{4\alpha^2}\right). \tag{73}$$

This solution is always damped. The root involving $\xi_-$ (see 70), also obtained when neglecting the $\mathcal{F}$ and $\mathcal{G}$ terms in the dispersion relation, is not large. It should therefore be discarded!

#### *4.4.2 Intermediate solutions*

These solutions have $|\upsilon| \sim 1$ and coincide with (64):

$$\upsilon = -\frac{\mathrm{i}\ell_\parallel^2}{8\alpha} \pm \sqrt{\mathcal{F} - \frac{\ell_\parallel^4}{64\alpha^2}}. \tag{74}$$

This is a pure firehose mode that goes unstable when $\mathcal{F} < 0$. If one looks at the dispersion relation in the form (56) one sees that this is a reasonable approximation as long as

$$\frac{\xi_-}{\xi_+}\,|\mathcal{G}-\mathcal{F}| \simeq \frac{\ell_\parallel^2}{4\alpha^2}\,|\mathcal{G}-\mathcal{F}| \simeq \frac{\ell_\parallel^2}{\alpha}\,\frac{\mathcal{M}}{\sqrt{16\pi\beta_\parallel}} \ll 1. \tag{75}$$

#### 4.4.3 Small solution

The small solution has $|\upsilon| \sim 1/\alpha \ll 1$. If we neglect the coupling term in (53) the small solution coincides with (63) with the plus sign, after expansion of the square root:

$$\upsilon = -\frac{\mathrm{i}\alpha}{2} + \sqrt{\mathcal{G}-\frac{\alpha^2}{4}} \simeq -\frac{\mathrm{i}\mathcal{G}}{\alpha}. \tag{76}$$

The approximation is for $|\mathcal{G}| \ll \alpha^2/4$. This mode goes unstable if $\mathcal{G} < 0$, so it is a pure mirror/firehose mode. This solution coincides with (67) and with (72) in the limit $\ell_\parallel^2\mathcal{G} \ll \alpha^2\mathcal{F}$. This shows how these solutions are connected across different wavelength/obliqueness regimes.

In the isotropic case $\mathcal{F} = \mathcal{G} = 1$ all solutions obtained above coincide with those found by Foote & Kulsrud (1979) for the corresponding values of $\alpha$ and $|\ell_\parallel|$.

The conclusion of this analysis is that for $\alpha \neq 0$ unstable modes occur for $\mathcal{F} < 0$ or for $\mathcal{G} < 0$, i.e. the same instability conditions that govern the low-$\beta$ firehose and mirror instabilities.

## 5 INSTABILITIES IN THE PRESENCE OF COSMIC RAYS

It is now commonly assumed that the bulk of the Galactic CRs obtains their energy through the process of diffusive shock acceleration, proposed by several authors around 1977/1978: Krymskii (1977), Axford, Leer & Skadron (1977), Bell (1978) and Blandford & Ostriker (1978). In this process, CRs cross a shock repeatedly and gain energy as a result of the velocity difference (net compression) between the up- and downstream flow. A still useful review of the basic theory is Drury (1983). Recent developments are reviewed by Schure et al. (2012). An essential ingredient of this theory is the presence of a turbulent magnetic field that provides the necessary scattering of the energetic particles, ties them to the fluid and allows them to tap the kinetic energy of the flow. Originally, it was thought that this scattering proceeds through the gyroresonant interaction with Alfvén waves, the process also thought to be responsible for the scattering of CRs in the Galactic interstellar medium. These are *self-generated* waves due to a streaming instability. It has been realized more recently (Bell & Lucek 2001; Bell 2004) that direct, non-resonant amplification of MHD waves is possible inside the CR precursor to the shock. This is usually referred to as the *Bell–Lucek instability*, BLI for short. The growth of the waves in this case is (mostly) generated by the current flowing in the bulk plasma (return current) rather than the direct CR current.

In the shock precursor created by shock-accelerated CRs (assumed to be protons for simplicity) there is a net charge and current density in the background (thermal) plasma. These are needed to compensate for charge- and current density of the CRs so that the total current- and charge density vanishes. In the rest frame of the plasma, to a good approximation the rest frame of the bulk of the ions, this charge- and current density is carried by the highly mobile electrons, and we have (e.g. Achterberg 1983; Bell 2004)

$$n_\mathrm{e} = n_\mathrm{i} + n_\mathrm{cr}, \quad en_\mathrm{e}u_\parallel = J_{\mathrm{cr}\parallel} \equiv en_\mathrm{cr}V_\mathrm{cr}. \tag{77}$$

Here $n_\mathrm{cr}$ is the density of CRs, and $J_{\mathrm{cr}\parallel}$ is the CR current along the magnetic field. The velocity $u_\parallel$ is the electron drift speed with respect to the ions. It is assumed that the shock propagates along the magnetic field.

It has been shown (Bell 2004; Luo & Melrose 2009) that the non-resonant instability occurs for wavelengths shorter than the CR gyration radius (i.e. for $r_\mathrm{g}^\mathrm{cr} \simeq pc/eB \gg 1/k_\parallel$ with $p = \gamma mc$ the CR momentum), which is much longer than the gyration radius $r_\mathrm{g}^\mathrm{i} \sim V_\perp/\Omega_\mathrm{i}$ of the thermal ions. In that limit the effect of the CR-induced current on the linear response of the background plasma changes wave properties much stronger than the *direct* response ($\boldsymbol{\chi}_\perp^\mathrm{cr}$) associated with the CRs themselves. Consequently the direct CR contribution to the plasma susceptibility can be neglected. As already discussed in Section 2.2, the electron current changes $\chi_{xy}^\mathrm{e}$ (see relation 32), the dominant electron contribution to the susceptibility. Adding the ion and electron contributions to $\chi_{xy}$ and using (77) one has

$$\chi_{xy} \simeq \mathrm{i}\frac{c^2}{V_\mathrm{A}^2}\,\frac{\beta_\parallel}{\nu}\left(\Delta_\mathrm{cr} + \frac{\ell_\parallel^2}{2\beta_\parallel} - \frac{3}{4}\,\frac{\ell_\perp^2}{\beta_\perp}\right), \tag{78}$$

with (in physical variables)

$$\Delta_\mathrm{cr} = \frac{n_\mathrm{cr}}{n_\mathrm{i}}\left(\frac{k_\parallel V_\mathrm{cr}}{\omega} - 1\right) \tag{79}$$

giving the effect of the CR-induced current. I have neglected a small term $\propto \Delta_T \sim 1/\beta$ in the ion susceptibility $\chi_{xy}^\mathrm{i}$ as well as the direct contribution $\chi_{xy}^\mathrm{cr}$ from the CRs.

On dimensional grounds one can define a typical wavenumber associated with the CR current:

$$k_\mathrm{cr} \equiv \frac{4\pi}{c}\,\frac{|J_{\mathrm{cr}\parallel}|}{B} = \frac{4\pi n_\mathrm{cr} e\,|V_\mathrm{cr}|}{cB}. \tag{80}$$

Its dimensionless counterpart, defined in terms of $k_0 = \Omega_\mathrm{i}V_\mathrm{A}/2V_\parallel^2$, is

$$\ell_\mathrm{cr} \equiv \frac{k_\mathrm{cr}}{k_0} = \beta_\parallel\,\frac{n_\mathrm{cr}}{n_\mathrm{i}}\left(\frac{|V_\mathrm{cr}|}{V_\mathrm{A}}\right). \tag{81}$$

In terms of $\ell_\mathrm{cr}$ expression (78) for $\chi_{xy}$ becomes

$$\chi_{xy} \simeq \mathrm{i}\frac{c^2}{V_\mathrm{A}^2}\left(\frac{\ell_\parallel^2}{2\nu} - \frac{3}{4}\,\frac{\beta_\parallel}{\beta_\perp}\,\frac{\ell_\perp^2}{\nu} + \sigma_\mathrm{cr}\,\frac{\ell_\mathrm{cr}|\ell_\parallel|}{\nu^2} - \frac{n_\mathrm{cr}}{n_\mathrm{i}}\,\frac{\beta_\parallel}{\nu}\right). \tag{82}$$

Here $\sigma_\mathrm{cr} = \mathrm{sign}(k_\parallel V_\mathrm{cr}) = \pm 1$. In CR precursors to a CR producing shock with velocity $V_\mathrm{s}$ one has

$$\frac{k_\parallel V_\mathrm{cr}}{\omega} \sim \frac{k_\parallel V_\mathrm{s}}{\omega} = \frac{k_\parallel V_\mathrm{A}}{\omega}\,\frac{V_\mathrm{s}}{V_\mathrm{A}} \gg \frac{k_\parallel V_\mathrm{A}}{\omega}, \tag{83}$$

as shock acceleration only proceeds efficiently if $V_\mathrm{s} \gg V_\mathrm{A}$. In that case one can safely neglect the last term inside the bracket in the expression for $\chi_{xy}$. I will use this approximation in what follows.

### 5.1 Combined firehose/Bell–Lucek instability

I will consider the parallel case $\ell_\perp = 0$. Dispersion relation (6) with (82) for $\chi_{xy}$ factors into

$$\left\{\upsilon^2 - \frac{|\ell_\parallel|}{2}\,\upsilon - \left(\mathcal{F}(\beta_\perp,\,\beta_\parallel) + \sigma_\mathrm{cr}\,\frac{\ell_\mathrm{cr}}{|\ell_\parallel|}\right)\right\} \times \left\{\upsilon^2 + \frac{|\ell_\parallel|}{2}\,\upsilon - \left(\mathcal{F}(\beta_\perp,\,\beta_\parallel) - \sigma_\mathrm{cr}\,\frac{\ell_\mathrm{cr}}{|\ell_\parallel|}\right)\right\} = 0. \tag{84}$$

The four solutions are $\upsilon = \pm\upsilon_+$, $\upsilon = \pm\upsilon_-$ with

$$\upsilon_\pm = \sqrt{\mathcal{F}(\beta_\perp,\ \beta_\parallel) + \sigma_{\rm cr}\,\frac{\ell_{\rm cr}}{|\ell_\parallel|} + \frac{\ell_\parallel^2}{16}} \pm \frac{|\ell_\parallel|}{4}. \tag{85}$$

There are unstable solutions with $\mathrm{Im}(\upsilon) > 0$ if the expression inside the two square roots turns negative, i.e. for

$$\mathcal{F}(\beta_\perp,\ \beta_\parallel) + \frac{\ell_\parallel^2}{16} \pm \sigma_{\rm cr}\,\frac{\ell_{\rm cr}}{|\ell_\parallel|} < 0. \tag{86}$$

In terms of physical variables:

$$1 + \frac{4\pi\left(P_\perp - P_\parallel\right)}{B^2} + \frac{\pi P_\parallel}{B^2}\left(\frac{k_\parallel V_\parallel}{\Omega_{\rm i}}\right)^2 \pm \sigma_{\rm cr}\,\frac{4\pi|J_{\rm cr\parallel}|}{|k_\parallel| cB} < 0. \tag{87}$$

For $\ell_{\rm cr} \ll 1$, $|\ell_\parallel| \ll 1$ so that finite Larmor radius effects can be neglected, and for an isotropic plasma with $\mathcal{F}(\beta_\perp,\ \beta_\parallel) = 1$, the four solutions of (85) reduce to the ones derived by Bell (2004), see his equation (15). In physical variables:

$$\omega_\pm = \pm V_{\rm A}\sqrt{k_\parallel^2 - |k_\parallel|\,k_{\rm cr}}. \tag{88}$$

In this limit an instability occurs with $\mathrm{Im}(\omega_+) > 0$ in the wavenumber range $0 < |k_\parallel| < k_{\rm cr}$, with the maximum growth rate at $|k_\parallel| = k_{\rm cr}/2$ that equals

$$(\mathrm{Im}(\omega))_{\rm max} = \frac{k_{\rm cr} V_{\rm A}}{2}. \tag{89}$$

In what follows I will look at the more general case. An instability will occur first in the solution for which the last term in (86/87) is negative, i.e. for $\pm\sigma_{\rm cr} = -1$. This case, where the CR-induced current is destabilizing, is considered now in more detail.

### 5.1.1 *Firehose-unstable case*

For the firehose-unstable case, $\mathcal{F} < 0$, one can define two new characteristic dimensionless wavenumbers

$$\ell_* \equiv \frac{4\sqrt{|\mathcal{F}|}}{\sqrt{3}},\quad \tilde{\ell}_{\rm cr} \equiv 2\,\ell_{\rm cr}^{1/3}, \tag{90}$$

and the associated auxiliary parameters

$$y \equiv \frac{|\ell_\parallel|}{\tilde{\ell}_{\rm cr}} = \frac{|\ell_\parallel|}{2\ell_{\rm cr}^{1/3}},\quad \eta = \frac{\ell_*}{\tilde{\ell}_{\rm cr}} = \frac{2\sqrt{|\mathcal{F}|}}{\sqrt{3}\,\ell_{\rm cr}^{1/3}}. \tag{91}$$

Instability condition (86) for $\pm\sigma_{\rm cr} = -1$ becomes

$$F(y) \equiv y^3 - 3\eta^2\,y - 2 < 0. \tag{92}$$

Standard analysis of this cubic equation (e.g. Abramowitz & Stegun 1970, Ch. 3.8) quickly establishes the following: as $y \geq 0$ by definition and with $F(0) = -2$ negative, $F(y)$ has a single negative minimum for $y > 0$ and a single positive root $y_{\rm m}$ of $F(y_{\rm m}) = 0$. The instability therefore occurs for $0 < y < y_{\rm m}$, with $y_{\rm m}$ given by

$$y_{\rm m} = \begin{cases} (1+\sqrt{1-\eta^6})^{1/3} + (1-\sqrt{1-\eta^6})^{1/3} & (0 \leq \eta < 1), \\ 2 & (\eta = 1), \\ \simeq\sqrt{3}\,\eta + \frac{1}{3\eta^2 + \frac{\sqrt{3}}{2\eta}} & (\eta > 1). \end{cases} \tag{93}$$

The first two relations, valid for $\eta \leq 1$, are exact. The approximate relation for $\eta > 1$ is obtained through twice iterating the relation $F(y) = 0$ for $y_{\rm m}$ in the form

$$y = \sqrt{3}\,\eta + \frac{2}{y\,(y + \sqrt{3}\,\eta)}, \tag{94}$$

treating the second term on the right-hand side as small and starting at $y = y_{(0)} = \sqrt{3}\,\eta$. This approximation is already very accurate at $\eta = 1$, where the exact solution is $y_{\rm m} = 2$: it gives $y_{\rm m} \simeq 1.991$.

### 5.1.2 *Firehose-stable case*

Here unstable solutions only occur for those modes where the last term on the left-hand side of (86)/(87) is negative, i.e. for $\pm\sigma_{\rm cr} = -1$. This instability is driven entirely by the CR-induced current, and corresponds most closely to the instability discussed by Bell (2004) and by Luo & Melrose (2009). They consider the case $\mathcal{F} = 1$ and neglect the finite Larmor radius terms.

With $\mathcal{F} \geq 0$ one can perform a similar analysis as in the previous case by defining $\tilde{\eta} = 2\sqrt{\mathcal{F}}/\sqrt{3}\,\ell_{\rm cr}^{1/3}$. The variable $y$ is defined as before: $y = |\ell_\parallel|/2\ell_{\rm cr}^{1/3}$. In these variables the instability condition now reads

$$\tilde{F}(y) \equiv y^3 + 3\tilde{\eta}^2\,y - 2 < 0. \tag{95}$$

One finds that a current-driven instability can occur for $0 < y < y_{\rm m}$ with

$$y_{\rm m} = (\sqrt{1+\tilde{\eta}^6}+1)^{1/3} - (\sqrt{1+\tilde{\eta}^6}-1)^{1/3}. \tag{96}$$

For very large $\tilde{\eta}$ one finds that $y_{\rm m}$ is small (i.e. a weak instability): $y_{\rm m} \approx 2/3\tilde{\eta}^2$. This corresponds to

$$|\ell_\parallel|_{\rm m} = \frac{\ell_{\rm cr}}{\mathcal{F}}\quad \left(|k_\parallel|_{\rm m} = \frac{k_{\rm cr}}{\mathcal{F}}\right), \tag{97}$$

and the dispersion relation in this limit is in physical variables

$$\omega \simeq \pm V_{\rm A}\sqrt{k_\parallel^2\mathcal{F} - |k_\parallel| k_{\rm cr}}. \tag{98}$$

### 5.1.3 *Firehose-unstable case with adverse current*

When $\mathcal{F} < 0$ and $\pm\sigma_{\rm cr} = +1$ there is the possibility of an instability that is 'pure firehose' in the sense that the CR-induced current is now stabilizing. Again using the variables defined in (90)/(91) the instability occurs when

$$\bar{F}(y) \equiv y^3 - 3\eta^2\,y + 2 < 0. \tag{99}$$

It is easily checked that $\bar{F}(y)$ has a minimum at $y = \eta$, where $\bar{F}(\eta) = 2(1-\eta^3)$. Therefore, an instability can only occur for $\eta > 1$, or equivalently

$$|\mathcal{F}(\beta_\perp,\ \beta_\parallel)| > \frac{3}{4}\,\ell_{\rm cr}^{2/3}. \tag{100}$$

In that case there are two positive real roots of $\bar{F}(y) = 0$, say $y_1$ and $y_2$, and an instability occurs for $y_1 < y < y_2$. Unfortunately, $y_1$ and $y_2$ are not readily calculated by analytic means, except in the case where $\eta \gg 1$ ($\ell_{\rm cr} \ll |\mathcal{F}|^{3/2}$) where $y_1 \simeq 2/3\eta^2 \ll 1$ and $y_2 \simeq \sqrt{3}\,\eta \gg 1$. In that limit an instability occurs in the wavenumber range

$$\ell_1 \simeq \frac{\ell_{\rm cr}}{|\mathcal{F}|} < |\ell_\parallel| < \ell_2 \simeq 4|\mathcal{F}|^{1/2}, \tag{101}$$

and the solutions of the dispersion relation in physical variables can be approximated by $\omega = \pm\omega_+, \pm\,\omega_-$ with

$$\omega_\pm = |k_\parallel| V_{\rm A}\sqrt{\frac{k_{\rm cr}}{|k_\parallel|} + \frac{k_\parallel^2 V_\parallel^4}{4\Omega_{\rm i}^2 V_{\rm A}^2} - |\mathcal{F}|} \pm \frac{k_\parallel^2 V_\parallel^2}{2\Omega_{\rm i}}. \tag{102}$$

Figs 3, 4 and 5 show the growth rate of the Firehose/BL Instability for increasing strength of the cr-induced current.

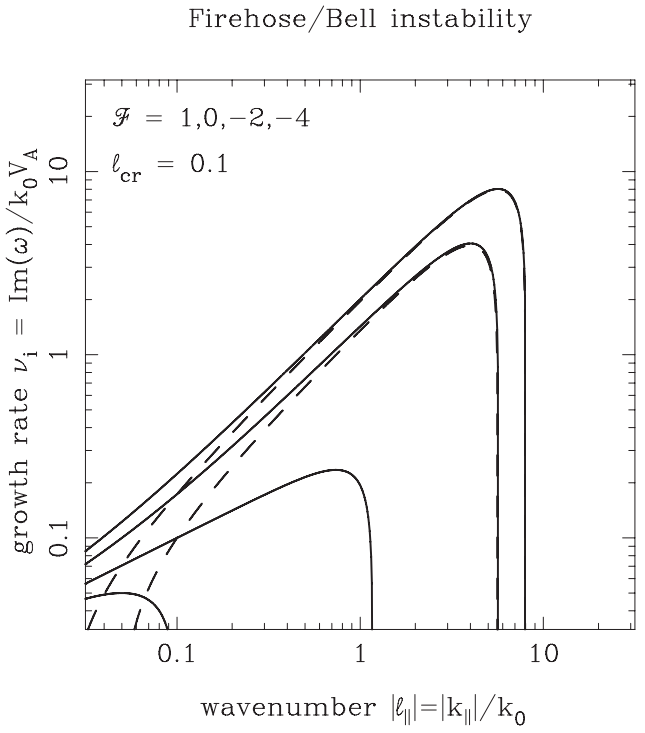


**Figure 3.** The dimensionless growth rate $\nu_i = \mathrm{Im}(\omega)/k_0V_A$ as function of the dimensionless wavenumber $|\ell_\parallel| = |k_\parallel|/k_0$. This figure is for $\ell_{cr} = 0.1$ (small CR-induced current) and for $\mathcal{F} = 1$, 0, −2 and −4. The solid curves give the growth rate for the most unstable modes that have $\pm\sigma_{cr} = -1$. These modes correspond to the case discussed by Bell (2004), and are unstable even when the classical firehose instability is absent for $\mathcal{F} \geq 0$. The two dashed curves correspond to modes with $\pm\sigma_{cr} = +1$, where the firehose mechanism for $\mathcal{F} < 0$ drives the modes unstable if condition (100) is satisfied.

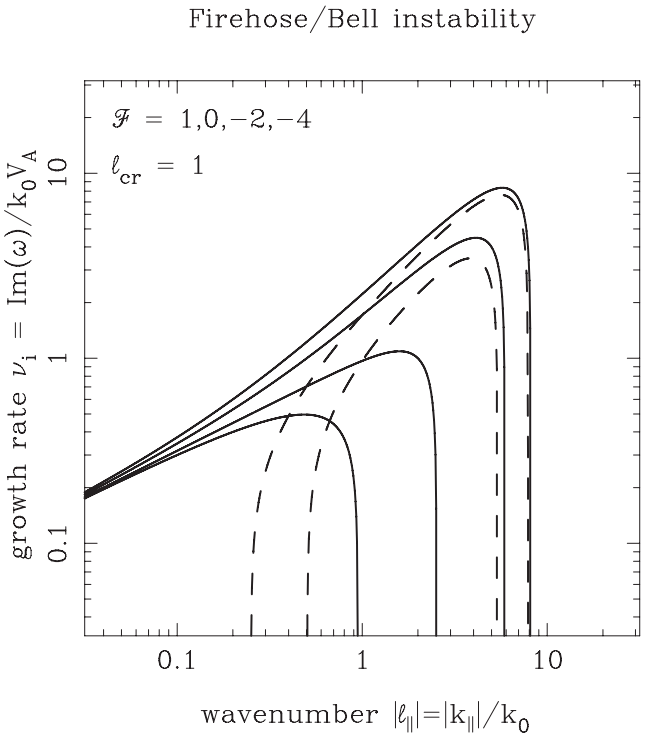


**Figure 4.** The same as Fig. 3, but now for a larger CR-induced current: $\ell_{cr} = 1$. There is an increase of the growth rate of the most unstable modes (solid curves, $\pm\sigma_{cr} = -1$) for $\ell_\parallel \lesssim \ell_{cr}$ due to the larger effect of the CR-induced current. On the other hand, the range of unstable wavenumbers is reduced by CR effects for the firehose unstable ($\mathcal{F} = -2$ and −4) modes with $\pm\sigma_{cr} = +1$, represented by the dashed curves.

### 5.2 Oblique propagation: combined mirror/Bell–Lucek instability

For oblique propagation ($k_\perp \neq 0$), the mirror instability becomes important if $P_\perp > P_\parallel$. Its dispersion relation is most straightforward in the low-frequency limit: $(\omega/kV_A)^2 \ll 1$. In that limit we have $\upsilon \simeq -\mathrm{i}\mathcal{G}/\alpha$ (cf. relation 67), in physical variables

$$\frac{\omega}{|k_\parallel|V_A} = -\mathrm{i}\left(\frac{k_\parallel}{k_\perp}\right)^2\left(\frac{\beta_\parallel}{\beta_\perp}\right)^2\frac{\mathcal{G}\left(\beta_\perp,\,\beta_\parallel\right)}{\sqrt{\pi\beta_\parallel}}. \tag{103}$$

The function $\mathcal{G}\left(\beta_\perp,\,\beta_\parallel\right)$ has been defined in (54) for the case $J_{cr} = 0$. Including the effects of the return current it becomes

$$\mathcal{G}\left(\beta_\perp,\beta_\parallel\right) = \left[1+\frac{\beta_\perp-\beta_\parallel}{2}\right]+\left(\frac{k_\perp}{k_\parallel}\right)^2\left[1+\beta_\perp\left(1-\frac{\beta_\perp}{\beta_\parallel}\right)\right] - \frac{k_{cr}^2}{k_\parallel^2\left(1+\dfrac{\beta_\perp-\beta_\parallel}{2}\right)}. \tag{104}$$

The instability condition $\mathrm{Im}(\omega) > 0$ requires $\mathcal{G}\left(\beta_\perp,\,\beta_\parallel\right) < 0$, in physical variables

$$k_\parallel^2\left[1+\frac{4\pi\left(P_\perp-P_\parallel\right)}{B^2}\right]+k_\perp^2\left[1+\frac{8\pi P_\perp}{B^2}\left(1-\frac{P_\perp}{P_\parallel}\right)\right] - \frac{k_{cr}^2}{1+\frac{4\pi\left(P_\perp-P_\parallel\right)}{B^2}} < 0. \tag{105}$$

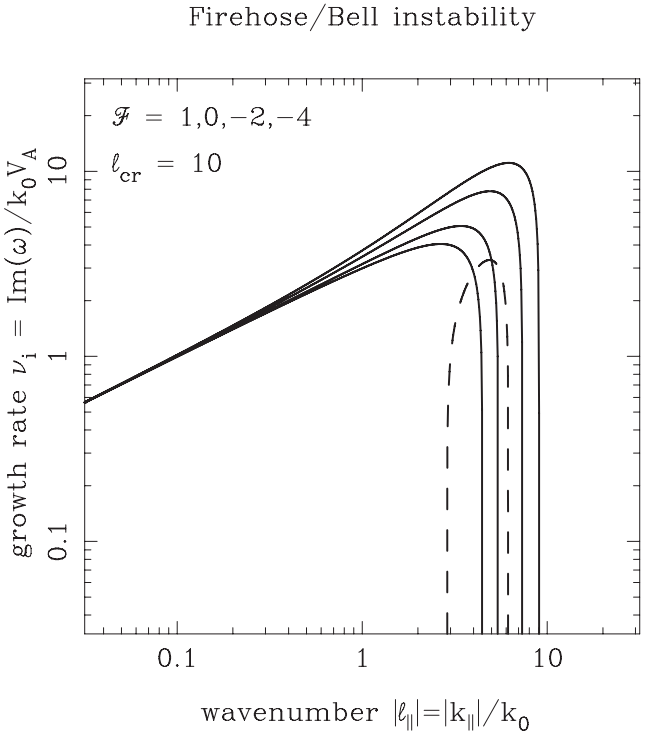


**Figure 5.** The same as Figs 3 and 4, but now for a large CR-induced current corresponding to $\ell_{cr} = 10$. The growth rate of the most unstable modes (solid curves, $\pm\sigma_{cr} = -1$) increases further. Of the modes with $\pm\sigma_{cr} = -1$ only the case $\mathcal{F} = -4$ is driven unstable by the firehose mechanism (dashed curve) over a limited wavenumber range.

One sees from condition (105) that the effect of the CR-induced return current is destabilizing *provided* that $\mathcal{F} = 1 + \left(\beta_\perp - \beta_\parallel\right)/2 > 0$, that is when the condition for the ordinary firehose instability is not satisfied.

For large $\beta$ and small pressure anisotropies, with $\beta_\perp = \beta\left(1 + \frac{1}{3}\Delta_T\right)$, $\beta_\parallel = \beta\left(1 - \frac{2}{3}\Delta_T\right)$ and $|\Delta_T| \ll 1$, one has to first order in $\Delta_T$ and $1/\beta$:

$$\mathcal{G}\left(\beta_\perp, \beta_\parallel\right) \simeq \frac{1}{k_\parallel^2}\left[(1-\beta\Delta_T)\,k_\perp^2 + \left(1+\frac{\beta\Delta_T}{2}\right)k_\parallel^2 - \frac{k_{\rm cr}^2}{1+\frac{\beta\Delta_T}{2}}\right]. \tag{106}$$

The instability condition $\mathcal{G}\left(\beta_\perp,\ \beta_\parallel\right) < 0$ then leads to the following condition when $\Delta_T > 0$ and $k_\perp > k_\parallel/\sqrt{2}$:

$$\beta\Delta_T > \frac{2k_\parallel^2 - k_\perp^2}{2k_\perp^2 - k_\parallel^2} + \frac{\sqrt{9k_\perp^4 - 4k_{\rm cr}^2\left(2k_\perp^2 - k_\parallel^2\right)}}{2k_\perp^2 - k_\parallel^2}. \tag{107}$$

Since $k_{\rm cr} \propto J_{\parallel{\rm cr}}$ the current needed to drive this mirror/Bell–Lucek branch unstable becomes smaller with increasing $\Delta_T$ and decreasing $k_\parallel/k_\perp$. When the return current is absent so that $k_{\rm cr} = 0$ condition (107) reduces to the instability condition implicit in the results derived by Schekochihin et al. (2005), as discussed in Section 3, equation (66).

If there is no pressure anisotropy at all ($\Delta_T = 0$) we get a slow-mode version of the BLI for $k = \sqrt{k_\perp^2 + k_\parallel^2} < k_{\rm cr}$, with a growth rate $\sigma \equiv {\rm Im}(\omega)$ equal to

$$\sigma = |k_\parallel| V_{\rm A}\,\frac{k_{\rm cr}^2 - k^2}{\sqrt{\pi\beta}\,k_\perp^2}. \tag{108}$$

The results in this subsection have not been obtained in earlier treatments that use cold plasma theory in the description of the wave response of the background plasma. That approach does not include kinetic effects, and in particular those associated with the Landau pole in the dispersion relation. In fact, the high-$\beta$ case considered here can only be done consistently using kinetic theory.

## 6 EFFECTS OF A FINITE ELECTRON TEMPERATURE ANISOTROPY

So far we have assumed that the temperature anisotropy in the electrons is vanishingly small, of order $\sqrt{m_{\rm e}/m_{\rm i}}\times$ the ion temperature anisotropy as a result of the more rapid electron–electron scattering, so that it can be neglected. In that case no terms involving the electron temperature appear in the dispersion relation. If we relax that assumption, additional electron terms involving the electron temperature anisotropy appear. Here I briefly consider their effect.

Defining the electron anisotropy parameter in the same fashion as for ions, $\tilde{\Delta}_T \equiv T_{\perp{\rm e}}/T_{\parallel{\rm e}} - 1$, the leading terms in the electron susceptibility are (compare 31, using $\omega_{\rm pe}^2/\Omega_{\rm e}^2 = m_{\rm e}c^2/m_{\rm p}V_{\rm A}^2$)

$$\chi_{xx}^{\rm e} \simeq \frac{m_{\rm e}}{m_{\rm p}}\,\frac{c^2}{V_{\rm A}^2}\left(\frac{\tilde{\omega}^2}{\omega^2} - \tilde{\Delta}_T\,\frac{k_\parallel^2 V_{\rm e}^2}{\omega^2}\right),$$

$$\chi_{yy}^{\rm e} \simeq \frac{m_{\rm e}}{m_{\rm p}}\,\frac{c^2}{V_{\rm A}^2}\left(\frac{\tilde{\omega}^2}{\omega^2} + \tilde{\Delta}_T\,\frac{(2k_\perp^2 - k_\parallel^2)V_{\rm e}^2}{\omega^2}\right)$$
$$+ \sqrt{2\pi}\,{\rm i}\,\frac{\omega_{\rm pe}^2}{\Omega_{\rm e}^2}\,\frac{k_\perp^2 V_{\rm e}^2}{\omega^2}\,\frac{\tilde{\omega}}{|k_\parallel|V_{\rm e}}\exp\left(-\frac{\tilde{\omega}^2}{k_\parallel^2 V_{\rm e}^2}\right),$$

$$\chi_{xy}^{\rm e} = -\chi_{yx}^{\rm e} \simeq -{\rm i}\,\frac{\omega_{\rm pe}^2\,\tilde{\omega}}{\omega^2|\Omega_{\rm e}|}. \tag{109}$$

Here I have neglected the electron temperature anisotropy in the factors multiplying $\tilde{\Delta}_T$, simply writing $V_{\rm e}^2 \equiv k_{\rm b}T_{\rm e}/m_{\rm e}$ for $V_{\perp{\rm e}}^2$ and for $V_{\parallel{\rm e}}^2$, under the assumption that $\tilde{\Delta}_T \sim \Delta_T \sim \beta^{-1} \ll 1$. This amounts to neglecting small corrections of order $\tilde{\Delta}_T^2$. I also neglected terms of order $k_\parallel^2 V_{\rm e}^2/\Omega_{\rm e}^2$, $k_\perp^2 V_{\rm e}^2/\Omega_{\rm e}^2$ with respect to unity.

One can use electron susceptibility (109) in the dispersion relation, neglecting the Landau term (the last term) in the expression for $\chi_{yy}^{\rm e}$, a good approximation for low-frequency waves as long as $T_{\rm e} \simeq T_{\rm i}$. For the wave modes discussed above in Sections 3– the only effect is that one should make the replacement

$$\Delta_T \implies \Delta_T + \left(\frac{T_{\rm e}}{T_{\rm i}}\right)\tilde{\Delta}_T. \tag{110}$$

The electrons terms not explicitly involving $\tilde{\Delta}_T$ in $\chi_{xx}^{\rm e}$ and $\chi_{yy}^{\rm e}$ are small (of order $m_{\rm e}/m_{\rm p}$) and can be neglected, as was argued already in Section 2.2. A more general discussion for strong electron temperature anisotropies can be found in Hellinger (2009).

## 7 THE NEED FOR HIGH $\beta$ AND LOW ION COLLISIONALITY FOR INSTABILITIES IN CR PRECURSORS

Pressure anisotropies in the bulk plasma typically change the properties of low-frequency (quasi-MHD) waves when

$$|\Delta P| \equiv \left|P_\perp - P_\parallel\right| > B^2/4\pi = 2P/\beta. \tag{111}$$

Such a situation is easy to achieve in a high-$\beta$ plasma. The scale $L_{\rm cr}$ of pressure gradients in the precursor that cause a pressure anisotropy is set by the diffusivity of the CRs. If they diffuse along the magnetic field with diffusion coefficient $\kappa_{\rm cr}$, that scale is $L_{\rm cr} \sim \kappa_{\rm cr}/V_{\rm s}$, with $V_{\rm s}$ the shock speed. In the shock rest frame $V_{\rm s}$ is the speed of the upstream plasma well ahead of the shock. In that frame one may assume a steady state, where the mass flux $\mathcal{J} \equiv \rho U_{\rm n}$ and the momentum flux $\rho U_{\rm n}^2 + P + P_{\rm cr}$ normal to the shock are both conserved. Here $\rho$ is the mass density of the ambient medium, $U_{\rm n}$ ($U_{\rm n} = V_{\rm s}$ for a normal shock) is the flow velocity component perpendicular to the shock, $P$ is the gas pressure and $P_{\rm cr}$ is the CR pressure. These simple relations neglect the pressure anisotropies in the ambient gas, assumed to be small (of order $1/\beta \ll 1$) in what follows, and magnetic stresses that are formally also of order $1/\beta$. This will suffice for order-of-magnitude estimates in the case of high Mach number shocks, precisely those shocks associated with the young supernova remnants of Type II (core-collapse) supernovae that are believed to be the sources of Galactic CRs.

In such shocks, where the shock speed is much larger than the (pre-shock) sound speed as well as the Alfvén speed, magnetic flux conservation gives $B_{\rm n}$ = constant and the induction equation in the MHD approximation gives $B_{\rm t}/\rho \simeq$ constant. Here $B_{\rm n}$ ($B_{\rm t}$) are the magnetic field components normal to (tangential to) the shock surface. If one neglects the effect of heat conduction the parallel and perpendicular pressures satisfy $P_\perp \propto \rho B$ and $P_\parallel \propto \rho^3/B^2$, the well-known Chew–Goldberger–Low relations for an anisotropic plasma (Chew, Goldberger & Low 1956). For small pressure anisotropies, where $P_\perp = P + \frac{1}{3}\Delta P$ and $P_\parallel = P - \frac{2}{3}\Delta P$ with $\Delta P \sim P/\beta \ll P$, the evolution of the pressure anisotropy in the ions is approximately described by

$$\left(\frac{\partial}{\partial t} + (\boldsymbol{U}\cdot\nabla)\right)\Delta P = 3P\left(\hat{\boldsymbol{b}}\hat{\boldsymbol{b}} : \nabla\boldsymbol{U} - \frac{1}{3}\nabla\cdot\boldsymbol{U}\right) - \nu_{\rm ii}\,\Delta P. \tag{112}$$

Here $\hat{\boldsymbol{b}} = \boldsymbol{B}/B$ is the unit vector along the magnetic field, $\boldsymbol{U}$ is the flow velocity and $\nu_{\rm ii}$ is the ion–ion collision frequency. The pressure anisotropy is only significant for the ions, since electron scattering proceeds a factor $\sqrt{m_{\rm i}/m_{\rm e}}(\simeq 43$ in a hydrogen plasma) faster for electrons. The first term on the right-hand side gives the generation of anisotropy due to changes in density and magnetic field strength, while the second term gives the relaxation of the anisotropy due to collisions. The notation $\hat{\boldsymbol{b}}\hat{\boldsymbol{b}} : \nabla \boldsymbol{U}$ is short-hand for $\hat{b}_i \hat{b}_j (\partial U_j/\partial x_i)$. If $x$ is the coordinate along the shock normal, and $i_B$ is the inclination angle of the magnetic field so that $B_{\rm n} = B\cos i_B$, balancing the generation term and the relaxation term gives an estimate for the pressure anisotropy:

$$\frac{\Delta P}{P} \simeq \frac{3\cos^2 i_B - 1}{\nu_{\rm ii}} \frac{{\rm d}U_{\rm n}}{{\rm d}x}, \tag{113}$$

where it is assumed that quantities in the precursor only depend on the normal coordinate $x$. If the flow inside the precursor is high Mach number, the increase of CR pressure towards the shock slows down the precursor flow according to $\mathcal{J}\,({\rm d}U_{\rm n}/{\rm d}x) \simeq -{\rm d}P_{\rm cr}/{\rm d}x$ over a scale $\Delta x \sim L_{\rm cr}$. Using as an estimate $|{\rm d}U_{\rm n}/{\rm d}x| \approx P_{\rm cr}/\mathcal{J}L_{\rm cr} = P_{\rm cr}/\rho V_{\rm s} L_{\rm cr}$, with $P_{\rm cr}$ the CR pressure at the shock, we have

$$\frac{|\Delta P|}{P} \simeq \frac{P_{\rm cr}}{\rho V_{\rm s} \nu_{\rm ii} L_{\rm cr}}. \tag{114}$$

Here I have put the geometrical factor involving $\cos^2 i_B$ to unity. For the pressure anisotropy to be important we need (see equation 111) $|\Delta P|/P > 2/\beta$. With (114) this condition can be written as a requirement on the precursor thickness $L_{\rm cr}$:

$$L_{\rm cr} < M_{\rm s} \left(\frac{\beta}{2}\right) \left(\frac{P_{\rm cr}}{\rho V_{\rm s}^2}\right) \lambda_{\rm i}. \tag{115}$$

Here $M_{\rm s} = V_{\rm s}/C_{\rm s}$ is the Mach number of the precursor flow with $C_{\rm s}$ the sound speed, and $\lambda_{\rm i} = V_{\rm i}/\nu_{\rm ii}$ is the scattering mean free path for ion–ion collisions with $V_{\rm i} = \sqrt{k_{\rm b} T_{\rm i}/m_{\rm i}}$ the ion thermal velocity for ion temperature $T_{\rm i}$. If electron and ion temperatures inside the precursor are not too different we have $V_{\rm i} \simeq C_{\rm s}$. Typical parameters for young Type II supernova blast waves that accelerate CRs and the surrounding interstellar medium are $M_{\rm s} \simeq 100$–$250$, $\beta \simeq 10$–$20$, $P_{\rm cr}/\rho V_{\rm s}^2 \simeq 0.1$. Requirement (115) typically leads to $L_{\rm cr}/\lambda_{\rm i} < 50$–$200$. The ion–ion scattering length is

$$\lambda_{\rm i} = \frac{V_{\rm i}}{\nu_{\rm ii}} \approx 10^{12} \left(\frac{n_{\rm i}}{1\,{\rm cm}^{-3}}\right)^{-1} \left(\frac{T_{\rm i}}{10^4\,{\rm K}}\right)^2 {\rm cm}. \tag{116}$$

The precursor scale is set by the CR diffusion coefficient and the shock speed:

$$L_{\rm cr} = \frac{\kappa_{\rm cr}}{V_{\rm s}} \approx 10^{14} \left(\frac{V_{\rm s}}{1000\,{\rm km\,s}^{-1}}\right)^{-1} \left(\frac{B}{3\,\mu{\rm G}}\right)^{-1} \eta\,\gamma_{\rm cr}\,{\rm cm}. \tag{117}$$

Here $\gamma_{\rm cr}$ is the typical Lorentz factor of the CRs contributing the bulk of the CR pressure, and $\eta = \kappa_{\rm cr}/\kappa_{\rm B}$ is the ratio of the CR diffusion coefficient and the Bohm diffusion coefficient $\kappa_{\rm B} = cr_{\rm g}/3$, with $r_{\rm g} = \gamma_{\rm cr} mc^2/qB$ the CR gyroradius. This last parameter is often assumed to be of order unity. If $\gamma_{\rm cr}$ is not too large and for young SNRs with $V_{\rm s} \simeq 3000\,{\rm km\,s}^{-1}$ it is fairly easy to satisfy condition (115). The numbers are for CR protons with $m = m_{\rm p}$ and $q = e$.

## 8 PRECURSOR STRUCTURE AND WAVE GENERATION

The magnitude and sign of the anisotropy depend on the orientation of the magnetic field in the precursor, see equation (112). I will consider the case of a high Mach number steady flow in the precursor, with $\boldsymbol{U} = U_{\rm n}(x)\,\hat{\boldsymbol{x}} + \boldsymbol{U}_{\rm t}$, where the shock is located at $x = 0$ and $x < 0$ ($x > 0$) corresponds the precursor region (post-shock flow). As long as $U_{\rm n} \gg V_{\rm A}$, precisely the condition for efficient acceleration of CRs, the density and magnetic field components normal and tangential to the shock scale in the precursor as

$$\rho(x) = r(x)\,\rho_0, \quad B_{\rm n} = B_{\rm n0}, \quad B_{\rm t} = r(x)\,B_{\rm t0}, \tag{118}$$

where $r(x)$ measures the compression inside the precursor. All quantities with subscript '0' refer to the conditions far ahead of the shock, formally at $x = -\infty$ where $r = 1$. In that case the geometrical factor in the anisotropy generation term in (112) scales as

$$3\cos^2 i_B - 1 = \frac{2 - r^2\,\tan^2 i_0}{1 + r^2\,\tan^2 i_0} \equiv \psi(r^2,\ i_0). \tag{119}$$

Here $i_0 \equiv i_B(x = -\infty)$ is the field inclination angle far ahead of the shock. Since $r(x) \geq 1$ increases monotonically with $x$, $\partial\psi/\partial\,(r^2) < 0$ and ${\rm d}U_{\rm n}/{\rm d}x < 0$ (decelerating flow) it follows that there are two possible cases.

(i) When $\tan^2 i_0 \geq 2$ we have $\psi(-\infty) \leq 0$ and $P_\perp - P_\parallel$ increases when one approaches the shock. Here only the mirror/BLI can occur.

(ii) When $\tan^2 i_0 < 2$ we have $\psi(-\infty) > 0$. In this case $P_\perp - P_\parallel$ first decreases, and the firehose/BLI instability can occur. If the approximations leading to (119) continue to hold this trend reverses if the compression in the precursor reaches a value where $r > \sqrt{2}/\tan i_0$. Depending on the circumstances one may get a mirror-unstable region closer to the shock.

The case $i_0 = 0$ (magnetic field along shock normal) is special: in that case $B_{\rm t} = 0$ throughout the precursor, $\psi = 2$ and only the firehose/BLI can occur.

As soon as the pressure anisotropy nears the level corresponding to the threshold for the (classical) firehose or mirror instability ($|\Delta P| \sim P/\beta$), one needs to use the full stress tensor $\boldsymbol{T}$ (including Reynolds stresses) that is appropriate for a gyrotropic plasma to describe precursor dynamics. In dyadic notation:

$$\boldsymbol{T} = \rho\,\boldsymbol{U}\boldsymbol{U} + P_\perp\,(\boldsymbol{I} - \hat{\boldsymbol{b}}\hat{\boldsymbol{b}}) + P_\parallel\,\hat{\boldsymbol{b}}\hat{\boldsymbol{b}} + P_{\rm cr}\,\boldsymbol{I} + \frac{B^2}{8\pi}\,\boldsymbol{I} - \frac{\boldsymbol{B}\boldsymbol{B}}{4\pi}. \tag{120}$$

Here $\boldsymbol{I} \equiv {\rm diag}(1,\ 1,\ 1)$ is the unit $3 \times 3$ tensor and $\hat{\boldsymbol{b}} \equiv \boldsymbol{B}/B$ is the unit vector along the magnetic field. Conservation (in a steady flow) of the momentum component normal to the shock, ${\rm d}T_{xx}/{\rm d}x = 0$, then reads

$$\rho U_{\rm n}^2 + \left(P_\perp + \frac{B^2}{8\pi}\right) \sin^2 i_B + \left(P_\parallel - \frac{B^2}{8\pi}\right) \cos^2 i_B + P_{\rm cr} = {\rm constant}. \tag{121}$$

When one nears the threshold of the classical firehose instability, $P_\parallel \simeq P_\perp + B^2/4\pi$, this reduces to $\rho U_{\rm n}^2 + P_\perp + P_{\rm cr} + (B^2/8\pi) \simeq$ constant. Near the threshold for the classical mirror instability, where $P_\parallel \simeq P_\perp^2/\left(P_\perp + \frac{B^2}{8\pi}\right) \simeq P_\perp - \frac{B^2}{8\pi}$ in a high-$\beta$ plasma, the momentum conservation law becomes approximately $\rho U_{\rm n}^2 + P_\perp + P_{\rm cr} - \psi\,(B^2/8\pi) \simeq$ constant with $\psi < 0$.

In both cases the bulk plasma in the precursor continues to decelerate under the influence of the adverse CR pressure gradient, and the instabilities described above are likely to occur.

## 9 CONCLUSIONS

In this paper I have considered the properties of low-frequency (quasi-MHD) waves in an anisotropic plasma using kinetic theory,

both without and with CRs present. In interstellar (or intracluster) gas with a sufficiently high ratio of kinetic to magnetic pressure, $\beta = 8\pi P/B^2$, only small pressure anisotropies are needed to produce an instability. At the same time, wave properties in these plasmas are more complex due to finite Larmor radius corrections scaling as $k_\perp^2 V_\perp^2/\Omega_i^2$ and the effect of thermal motion along the field that leads to corrections that scale as $k_\parallel^2 V_\parallel^2/\Omega_i^2$. I have shown that the well-known mirror and firehose instabilities persist in these plasmas. The only significant change in the condition for instability occur for the firehose instability in the case of pure parallel propagation, when $k_\perp = 0$. In that case finite Larmor radius corrections are stabilizing. For oblique propagation ($k_\perp \neq 0$) new modes appear whose stability is governed by the classical conditions $\mathcal{F} < 0$ (firehose instability) and $\mathcal{G} < 0$ (mirror instability). The frequency of the waves (both the stable and unstable modes) differs significantly from the MHD fluid results if the wavelength is sufficiently short, in terms of wavenumber: when $k = 2\pi/\lambda > k_0 = \Omega_i/V_A\beta_\parallel$.

I have also considered the interplay between the mirror and firehose instabilities and the return-current driven BLI that can occur in the precursor of accelerated particles (CR) that precedes a high Mach number shock in astrophysical plasmas. I have shown that the deceleration of the flow in the precursor due to the CR pressure increase towards the shock in fact generates a pressure anisotropy in the bulk plasma. This creates the possibility of a combined firehose/BLI for parallel propagation with respect to the magnetic field, or a mirror/BLI for oblique propagation. The most unstable modes of both instabilities exhibit a significantly larger growth rate and a larger range of unstable wavelengths compared to their counterparts in an isotropic plasma.

Simple estimates suggest that such conditions can exist where the ion–ion collisions in the thermal gas are not strong enough to keep the difference between the parallel and perpendicular pressures below the threshold for an instability. In those cases where such conditions prevail one expects more efficient magnetic field generation and, as a consequence, acceleration of CRs to higher energies since (for nuclei that suffer no radiation losses, and according to the simples models) the maximum attainable energy $\mathcal{E}_{max}$ typically scales as $\mathcal{E}_{max} \propto B$.

There are a number of effects that are potentially important that have not been considered in this paper. First of all it is possible that the pressure associated with the CRs is also anisotropic. This case has been considered recently by Schure & Bell (2011). Secondly, as the collisions in the bulk (thermal) plasma become less important, the effects of thermal conduction become stronger. The bi-Maxwellian model used here for the thermal plasma precludes the treatment of these effects. It does allow, however, a quick comparison with the results obtained earlier by Foote & Kulsrud (1979) for isotropic thermal (Maxwellian) plasmas.

## REFERENCES


Abramowitz M., Stegun I. A., 1970, Handbook of Mathematical Functions. Dover Press, New York

Achterberg A., 1983, A&A, 119, 274

Akhiezer A. I., Akhiezer I. A., Polovin R. V., Sitenko A. G., Stepanov K. N., 1975, Plasma Electrodynamics, Vol. 1. Pergamon Press, Oxford, Ch. 5

Axford W. I., Leer E., Skadron G., 1977, in International Cosmic Ray Conference, Vol. 11. Sofia, B'lgarska Akademiia na Naukite, Sofia, p. 132

Barnes A., 1966, Phys. Fluids, 9, 1483

Bell A. R., 1978, MNRAS, 182, 147

Bell A. R., 2004, MNRAS, 353, 550

Bell A. R., Lucek S. G., 2001, MNRAS, 321, 433

Blandford R. D., Ostriker J. P., 1978, ApJ, 221, L29

Chew G. F., Goldberger M. L., Low F. E., 1956, Proc. R. Soc. Lond. A, 236, 112

Drury L. O'C., 1983, Rep. Progress Phys., 46, 973

Foote E. A., Kulsrud R. M., 1979, ApJ, 233, 302

Hasegawa A., 1975, Plasma Instabilities and Nonlinear Effects. Springer-Verlag, Berlin

Hellinger P., 2009, Phys. Plasmas, 14, 082105

Ichimaru S., 1973, Basic Principles of Plasma Physics: A Statistical Approach. Benjamin, Reading, MA

Krymskii G. F., 1977, Akademiia Nauk SSR Doklady, 234, 1306

Lucek S. G., Bell A. R., 2000, MNRAS, 314, 65

Luo Q., Melrose D., 2009, MNRAS, 397, 1402

Schekochihin A. A., Cowley S. C., Kulsrud R. M., Hammett G. W., Sharma P., 2005, ApJ, 629, 139

Schekochihin A. A., Cowley S. C., Rincon F., Rosin M. S., 2010, MNRAS, 405, 291

Schure K. M., Bell A. R., 2011, MNRAS, 418, 782

Schure K. M., Bell A. R., Drury L. O'C., Bykov A. M., 2012, Space Sci. Rev., 173, 491

Southwood D. J., Kivelson M. G., 1993, J. Geophys. Res., 98, 9181

Stepanov K. N., 1958, Sov. Phys. JETP, 34, 892

Stix T. H., 1992, Waves in Plasmas. Am. Inst. Phys., New York, Ch. 10 and 11


This paper has been typeset from a TEX/LATEX file prepared by the author.